

## 2.3 GIS Database Generation

### 2.3.1 Administration and Sub-Basin Boundary Data

#### (1) Administration Boundaries

The definitions of administration boundary in Iran are as follows.

1. Province: several townships make a province
2. Township: several cities or town make a township
3. District: several villages make district
4. Rural district: Several villages and Rural make a rural district.

In the database, Administration boundary is generated from 1:25,000 scale topographic maps. The data is presented up to rural district. The image map of administration boundary is as follow.

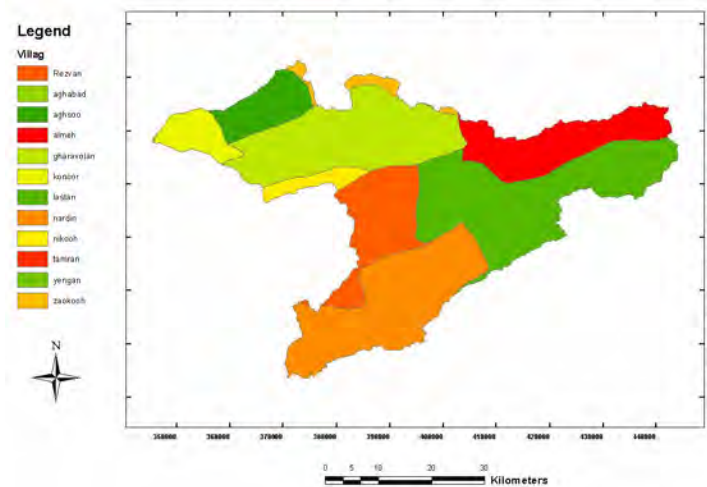


**Figure 2.10 Administration Boundary Map of Madarsoo River Basin**

#### (2) Basin Boundaries

The basin and its sub-basins' boundary of Madarsoo river have been extracted from 1:25,000 topographic maps by JICA study team. The basin contains 8 sub-basins.



**Figure 2.11 Image Map of Madarsoo River Basin**

The attribute table includes area and sub-basin ID. The Area item shows the area of each sub basin in  $m^2$ . The Basin\_ID item shows the number of each sub basin.

**Table 2.2 The Attribute table of Basin Boundary**

FD	Shape <sup>1</sup>	AREA	PERIMETER	basin_id
0	Polygon	136427792	64208.938	2
1	Polygon	361990688	119823.016	4
2	Polygon	94778400	59343.703	1
3	Polygon	451780864	113188.359	8
4	Polygon	281235648	76687.289	3
5	Polygon	126499672	63912.332	5
6	Polygon	787127104	200633.219	7
7	Polygon	125120328	50303.477	6

### 2.3.2 Social Economy Data

The social economy data includes Historical Cultural Tourism, Rainfall Hydro station and River Structures data.

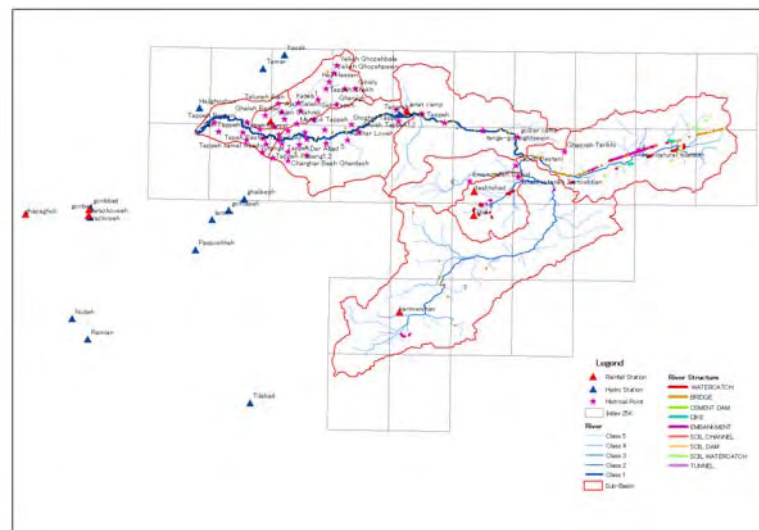


**Figure 2.12 Image Map of Social Economy Data**

(1) River Structures

The river structures are generated from 1:25,000 scale topographic map. All river structures, includes bridge and civil establishment are represented as points and lines. The type of the river structure is also included in the attribute table.

(2) Rainfall and Hydrological Stations

This is a point layer for displaying rainfall and hydrologic stations in the study area. There are 4 rainfall stations and one hydrology station in Tangrah. The attribute data includes name, elevation in meter, and mean of annual rainfall in mm.

(3) Historic, Cultural and Tourism Points

Environment specialist of JICA study team prepared this data. It includes the name of the point, type of the location according to historic, tourist and cultural use.

### 2.3.3 Natural Environment Data

The natural environment data includes Land use, Soil distribution, Natural Protect area, Rainfall distribution and Geology.

#### (1) Land Use

Land use and vegetation cover is a basis of watershed management. In order to prepare land use maps, the images of Land Sat ETM , IRS-LISSIII, PAN in 2002-2004 have been utilized. Other sources such as topographic maps, land use maps, past vegetation cover maps and field appraisal have been also utilized. The preparation steps are as follows.

1. Preparing satellite image.
2. Geo-referencing of the satellite image by GCP extracted from 1:25000 topographic maps.
3. Supervised and unsupervised and hybrid processing.
4. Omitting additional classes and aggregating small and big classes.
5. Testing primary map and preparing final map by sampling and comparing the equal coordinate with ground. Confusion matrix was extracted and Kappa (overall accuracy) coefficient was determined at 93 percent.

Class definition and brief description of this data is presented as follows.

#### (i) Agriculture Class

It contains fields for plants more than one year; water and rain feed planting tree and harvesting fields. The following sub classes have been extracted from this class.

1. Rain feed: contains the rain feed areas; these fields are usually located between steep slope regions and flat regions. Their annual rainfall is 400 millimeter. In most areas the ranges charge into rain feed fields due to their appropriate situation.
2. Agriculture: Contains the area in flat part and near flood plain.

#### (ii) Forest Class

Forests are the areas where the tree cover more than 10% and it influence on climate balance. The forest with less than 10% cover such as deforest area, intensive grazed forests or destroyed with any other reason are out of balance. They have no special use but they can be recovered. The forest class is divided as follows.

1. Dense: the cover is more than 70%
2. Semi- dense: the cover is between 40% and 70%
3. Low: the cover is less than 40 percent

#### (iii) Rangeland Class

The rangeland includes grass, bushes and so on. The ranges usually are used for grazing. The rangeland class is divided as follow.

1. Dense range: the ground cover is high (about 25% to 50%)
2. Semi- dense range: the ground cover is average about 10-25%
3. Low- dense range: the ground cover is low about 0 to 10%

(iv) Range- Rain Feed Class

It located in rain feed, it is used as rain feed lands but also contain semi-dense range.

(v) Range-Orchard Class

It contains lands where there are disperse gardens with range. Some parts of ground cover contains gardens along with seasonal and temporal rivers.

(vi) Urban Class

It contains dwelling houses, industrial areas, recreational facilities communication and so on.

(vii) Flood Plain Class

This class is always around down stream of the river.

(viii) Canopy Cover Class

This class is digitized from map that belongs to forests and ranges organization. But since canopy covers of ranges and forests have changed, the satellite image was used to get an accurate percent.

The land use map is shown in as follow.

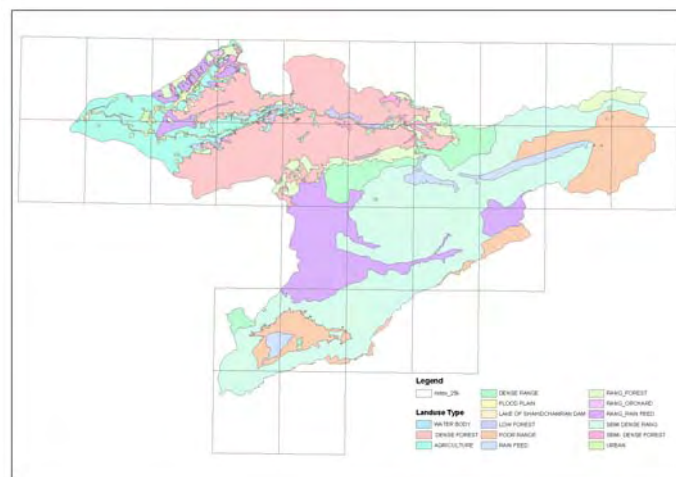


**Figure 2.13 Image Map of Land Use**

(2) Soil Distribution

The original data source for this data is 1:250,000 soil maps. The attribute table of this data includes following information.

1. Soil- type in Persian: shows the type of the soil in Persian
2. Soil- type in English: shows the type of the soil in English
3. Label: shows the code of land evaluation.
4. Describe: Description of each land evaluation code.



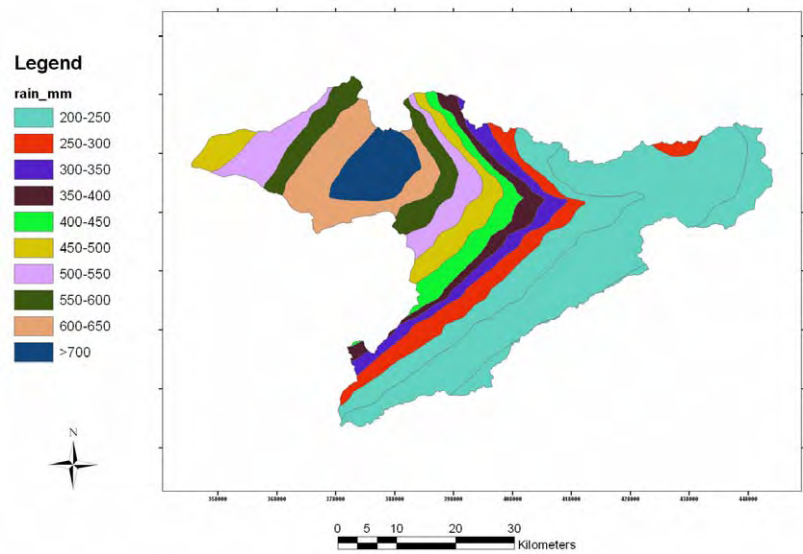


**Figure 2.16 Image Map of Annual Rainfall Distribution**

(5) Geology & Fault Line

This layer is prepared by digitizing 1:100,000 geology maps. All formations were put in database. Other information such as aspect, slope and Anticline–Syncline are also included in database. The image map is as follow.

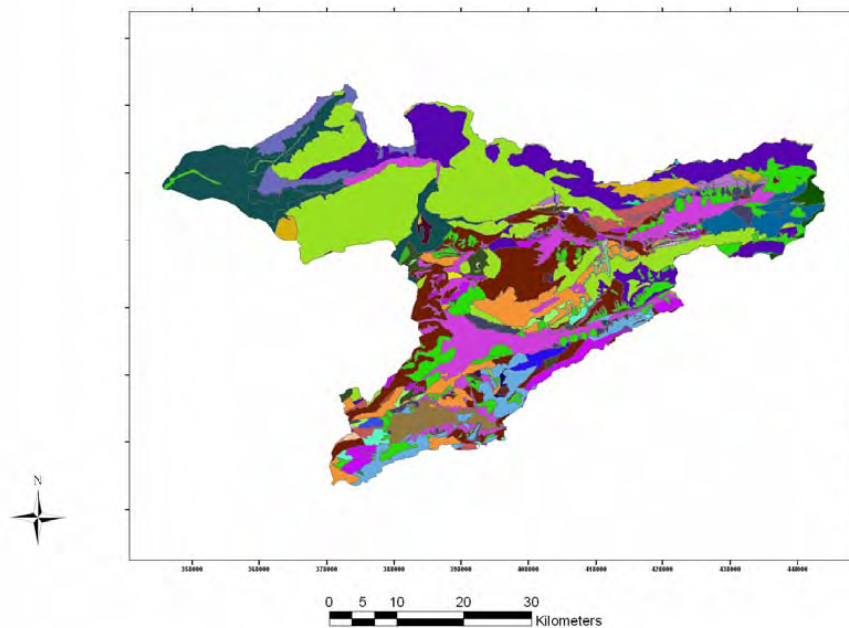


**Figure 2.17 Image Map of Geology**

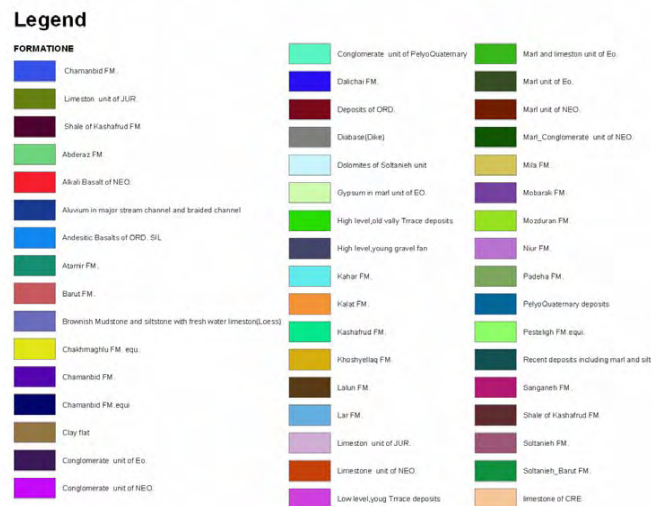


Figure 2.18 Legend of 30-formation of geology

### 2.3.4 Topographical Data

#### (1) Road Network

Road network was extracted from 1:25,000 topographic maps. This layer contains all accessible roads with different types. The types of road are determined by road conditions. The image map of road network is shown as follow.

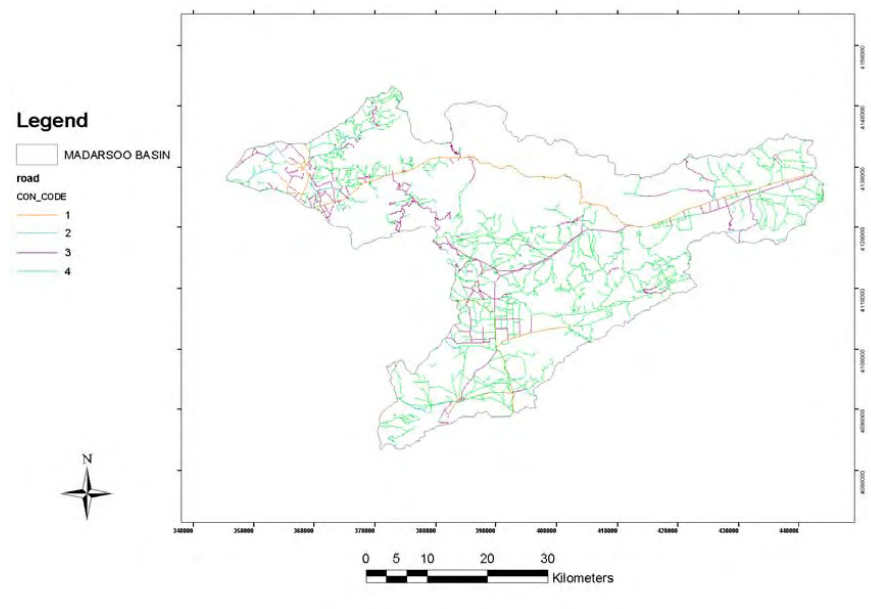


Figure 2.19 Image Map of Road Network

The attribute table includes following information.

1. Con-cod: this field shows road type and it based on the road conditions.
2. Describe: Description of each type that presented in Con-code field.
3. The information about road networks is as following table.

**Table 2.3 Attribute Table of Road Network**

FID	Shape	CON_CODE	DESCRIBE	شرح
39	Polylines	4	PEDSTRAN D RT ROAD	راه خاكي بياده رو
40	Polylines	4	PEDSTRAN D RT ROAD	راه خاكي بياده رو
41	Polylines	4	PEDSTRAN D RT ROAD	راه خاكي بياده رو
42	Polylines	4	PEDSTRAN D RT ROAD	راه خاكي بياده رو
43	Polylines	1	PAVED ROAD	راه آسفالتنه
44	Polylines	3	JEEP DIRT ROAD	راه خاكي جيب رو
45	Polylines	3	JEEP DIRT ROAD	راه خاكي جيب رو
46	Polylines	3	JEEP DIRT ROAD	راه خاكي جيب رو
47	Polylines	3	JEEP DIRT ROAD	راه خاكي جيب رو
48	Polylines	3	JEEP DIRT ROAD	راه خاكي جيب رو
49	Polylines	3	JEEP DIRT ROAD	راه خاكي جيب رو
50	Polylines	3	JEEP DIRT ROAD	راه خاكي جيب رو
51	Polylines	4	PEDSTRAN D RT ROAD	راه خاكي بياده رو
52	Polylines	4	PEDSTRAN D RT ROAD	راه خاكي بياده رو
53	Polylines	4	PEDSTRAN D RT ROAD	راه خاكي بياده رو
54	Polylines	3	JEEP DIRT ROAD	راه خاكي جيب رو
55	Polylines	3	JEEP DIRT ROAD	راه خاكي جيب رو
56	Polylines	3	JEEP DIRT ROAD	راه خاكي جيب رو
57	Polylines	3	JEEP DIRT ROAD	راه خاكي جيب رو
58	Polylines	3	JEEP DIRT ROAD	راه خاكي جيب رو
59	Polylines	3	JEEP DIRT ROAD	راه خاكي جيب رو
60	Polylines	3	JEEP DIRT ROAD	راه خاكي جيب رو
61	Polylines	4	PEDSTRAN D RT ROAD	راه خاكي بياده رو
62	Polylines	4	PEDSTRAN D RT ROAD	راه خاكي بياده رو
63	Polylines	4	PEDSTRAN D RT ROAD	راه خاكي بياده رو
64	Polylines	4	PEDSTRAN D RT ROAD	راه خاكي بياده رو
65	Polylines	3	JEEP DIRT ROAD	راه خاكي جيب رو
66	Polylines	4	PEDSTRAN D RT ROAD	راه خاكي بياده رو
67	Polylines	4	PEDSTRAN D RT ROAD	راه خاكي بياده رو
68	Polylines	4	PEDSTRAN D RT ROAD	راه خاكي بياده رو
69	Polylines	4	PEDSTRAN D RT ROAD	راه خاكي بياده رو
70	Polylines	4	PEDSTRAN D RT ROAD	راه خاكي بياده رو
71	Polylines	4	PEDSTRAN D RT ROAD	راه خاكي بياده رو

The definition of Describe item is as follows.

1. PAVED ROAD: Shows the roads that their surface is paved and are two-sided
  2. GRAVELLED ROAD: Shows the two-sided sandy and surface-constructed roads and more.
  3. JEEP DIRT ROAD: Shows the dirt roads where there is limitation for cars' movement
  4. PEDSRIAN DIRT ROAD: Shows the dirt roads where human being and cattle can just move.
- (2) River Network

This layer is extracted and digitized from 1:25,000 topographic maps. Since, river network is crucial in flood studies, the details are also presented in 1:25,000 maps. So the scale of river layer in database is 1:25,000.



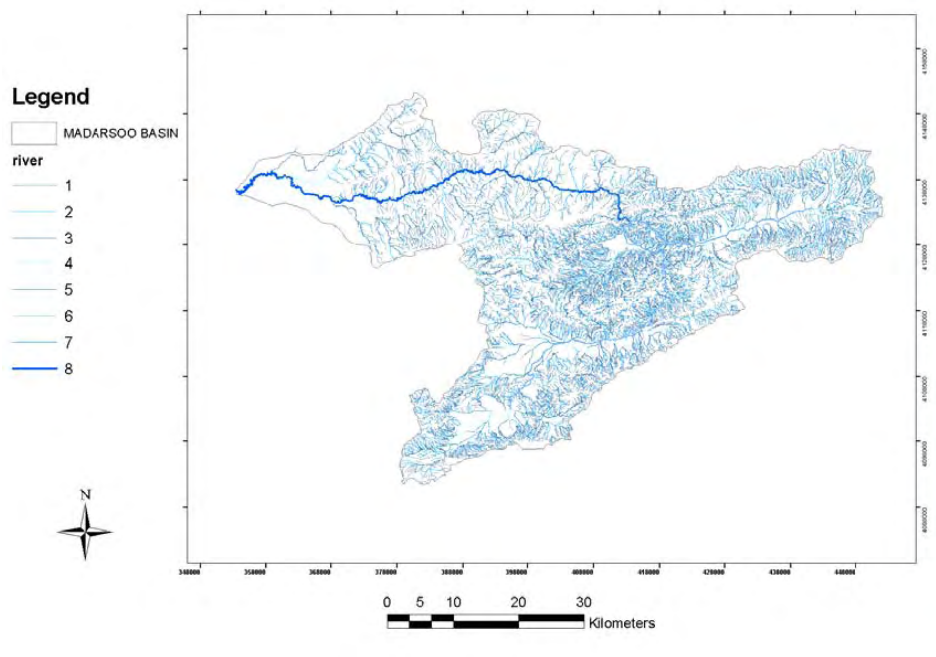


**Figure 2.20 Image Map of River Network**

The attribute data of this layer includes river name and class. It is as following table.

**Table 2.4 Attribute Table of River Network**

FID	Shape*	STR_order	NAME
4391	Polyline	6	
4397	Polyline	6	
4445	Polyline	6	
4464	Polyline	6	
4470	Polyline	6	
4494	Polyline	6	
4506	Polyline	6	
4567	Polyline	6	
4694	Polyline	6	
4746	Polyline	6	
4834	Polyline	6	
5166	Polyline	6	
5181	Polyline	6	
5200	Polyline	6	
5286	Polyline	6	
5314	Polyline	6	
5317	Polyline	6	
5380	Polyline	6	
5414	Polyline	6	
5494	Polyline	6	
5506	Polyline	6	
5527	Polyline	6	
5537	Polyline	6	
5539	Polyline	6	
5554	Polyline	6	
8112	Polyline	6	
8429	Polyline	6	
9857	Polyline	6	
9858	Polyline	6	
9859	Polyline	6	
10189	Polyline	7	
10190	Polyline	7	
564	Polyline	8	madarsoo

The table of this layer includes following information.

1. Name: the name of the rivers.
2. STR-order: Ranking of the river network. Main branch is the first class. There are 8 classes in this river network data.

(3) Water Body

This layer is extracted from 1:25,000 topographic maps. it contains small and big dams and lakes. The attribute data of this layer includes the Type of the water body in both English and Persian.

**Table 2.5 Attribute Table of Water Body**

FID	Shape	DESCRIBE	شرح
0	Polygon	Soil watercatch	آب بند خاکی
1	Polygon	Soil watercatch	آب بند خاکی
2	Polygon	Soil cam	سد خاکی
3	Polygon	Soil cam	سد خاکی
4	Polygon	Soil watercatch	آب بند خاکی
5	Polygon	watercatch	آب بند
6	Polygon	watercatch	آب بند
7	Polygon	watercatch	آب بند
8	Polygon	Soil cam	سد خاکی
9	Polygon	Soil cam	سد خاکی
10	Polygon	watercatch	آب بند
11	Polygon	watercatch	آب بند
12	Polygon	soil channel	کانال خاکی
13	Polygon	watercatch	آب بند
14	Polygon	shahid_chamran_dam_lake	سد شهید چمران
15	Polygon	WATER POOL	استخر آب
16	Polygon	WATER POOL	استخر آب
17	Polygon	WATER POOL	استخر آب
18	Polygon	WATER POOL	استخر آب
19	Polygon	WATER POOL	استخر آب
20	Polygon	WATER POOL	استخر آب
21	Polygon	shahid_chamran_dam_lake	سد شهید چمران
22	Polygon	golestan_dams_lake	سد گلستان
23	Polygon	watercatch	آب بند
24	Polygon	watercatch	آب بند
25	Polygon	watercatch	آب بند

(4) Build up Area

In order to make this layer in database, all populated areas were extracted from 1:25,000 topographic maps and satellite image. Since there are important establishments in the area, a layer called AS-BUILD-LINE was prepared and put in database. This new layer contains electricity, gas and water pipes that were extracted from 1:25,000 topographic maps.

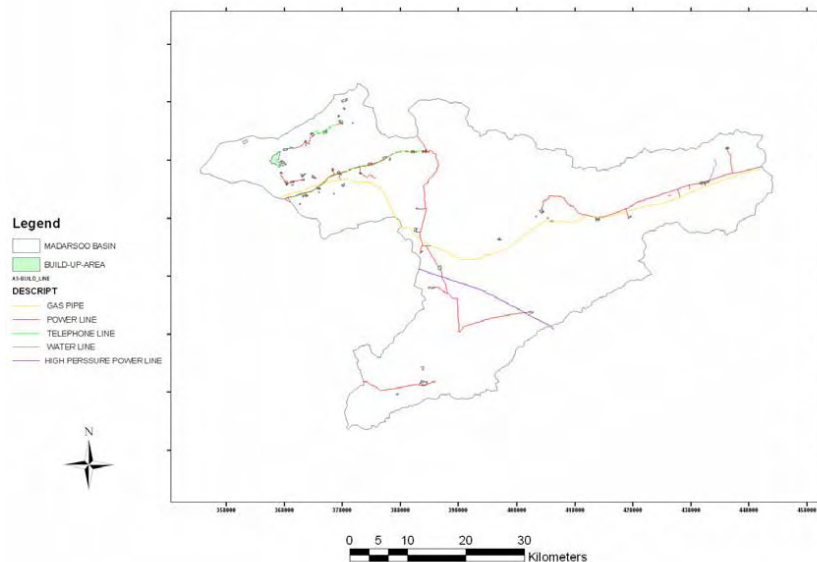


**Figure 2.21 Image Map of Built Up Area**

The table of BUILD-UP-AREA layer contains following information.

1. Name: contains the names of features
2. Type: contains the type of features.

**Table 2.6 Attribute Table of Built Up Area**

FID	Shape	NAME	نام
0	Polygon	Yeke_Ghooze Olva	یکه فوژ اولیا
1	Polygon	Yeke_Ghooze Sofla	یکه فوژ سفلا
2	Polygon	Haji Hassan	حاجی حسن
3	Polygon	Saleh Abad	صالح آباد
4	Polygon	Chadi Abad	چادی آباد
5	Polygon	Ghanjigh	قنجیق
6	Polygon	Ghanjigh	قنجیق
7	Polygon	Ghanjigh	قنجیق
8	Polygon	Ajen Sangdi	آجن سنگدی
9	Polygon	Bolook Ajen	بلوک آجن
10	Polygon	Cheyar Mazi	چیار مازی
11	Polygon	Cheyar Mazi	چیار مازی
12	Polygon	Ajen Yeli	آجن یلی
13	Polygon	Ghoochaman	فوجمن
14	Polygon	Shahrake Farhangiyar	شهرک فرهنگیان

The table of AS-BUILD-LINE contains following information.

1. ID: is the numerical code of features
2. Describe: Changing numeric codes into English and Persian

**Table 2.7 Attribute Table of As Build Line**

FID	Shape	ID	DESCRIBE	شرح
0	Polyline	2	POWER LINE	خطوط انتقال نیرو
1	Polyline	2	POWER LINE	خطوط انتقال نیرو
2	Polyline	2	POWER LINE	خطوط انتقال نیرو
3	Polyline	2	POWER LINE	خطوط انتقال نیرو
4	Polyline	7	POWER LINE	خطوط انتقال نیرو
5	Polyline	2	POWER LINE	خطوط انتقال نیرو
6	Polyline	2	POWER LINE	خطوط انتقال نیرو
7	Polyline	2	POWER LINE	خطوط انتقال نیرو
8	Polyline	2	POWER LINE	خطوط انتقال نیرو
9	Polyline	4	TELEPHONE LINE	خطوط تلفن
10	Polyline	2	POWER LINE	خطوط انتقال نیرو
11	Polyline	2	POWER LINE	خطوط انتقال نیرو
12	Polyline	2	POWER LINE	خطوط انتقال نیرو
13	Polyline	4	TELEPHONE LINE	خطوط تلفن
14	Polyline	2	POWER LINE	خطوط انتقال نیرو
15	Polyline	4	TELEPHONE LINE	خطوط تلفن
16	Polyline	2	POWER LINE	خطوط انتقال نیرو
17	Polyline	4	TELEPHONE LINE	خطوط تلفن
18	Polyline	5	WATER LINE	لوله آب
19	Polyline	2	POWER LINE	خطوط انتقال نیرو
20	Polyline	2	POWER LINE	خطوط انتقال نیرو
21	Polyline	2	POWER LINE	خطوط انتقال نیرو
22	Polyline	2	POWER LINE	خطوط انتقال نیرو
23	Polyline	1	HIGH PRESSURE POWER LINE	خط انتقال برق فشار قوی
24	Polyline	2	POWER LINE	خطوط انتقال نیرو
25	Polyline	2	POWER LINE	خطوط انتقال نیرو
26	Polyline	3	GAS PIPE	لوله گاز
27	Polyline	3	GAS PIPE	لوله گاز
28	Polyline	2	POWER LINE	خطوط انتقال نیرو
29	Polyline	2	POWER LINE	خطوط انتقال نیرو
30	Polyline	2	POWER LINE	خطوط انتقال نیرو
31	Polyline	2	POWER LINE	خطوط انتقال نیرو
32	Polyline	2	POWER LINE	خطوط انتقال نیرو

(5) Village

This layer is extracted from 1:25,000 topographic maps. The information of this layer contains name and type of village and their statistical data.

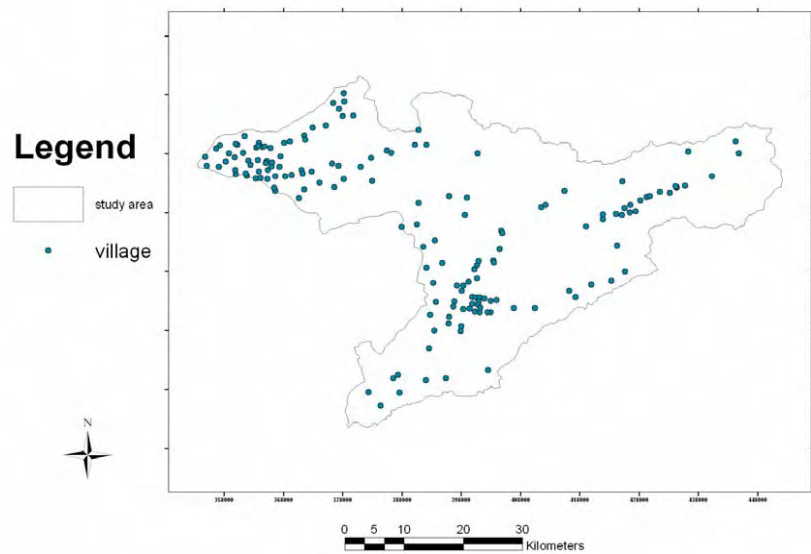


**Figure 2.22 Image Map of Village Point**

The attribute source was the booklet of village information prepared by management and planning organization of the province. It includes following information.

1. Village code: is prepared by statistic center of Iran
2. Village-name: it shows the name of the village.
3. House hold: Shows the house holds of the village or rural district.
4. Population: Shows the population of village or rural district.
5. Man: The number of men
6. Woman: The number of women
7. Age 6: The number of population from 6 to 9 years old.
8. Age 10: The number of 10 years old or above
9. Educated: The number of educated people
10. Employed: The number of employed people
11. Unemployed: The number of unemployed people
12. Medical center: The number of medical centers
13. Pharmacy: The number of pharmacies
14. Health-care center: The number of health-care centers
15. Bath: The number of baths
16. Security guard: The number of security guards
17. Cooperative society: The number of cooperative societies
18. Rural services: The number of rural services
19. Telephone: The number of telephone facilities
20. Telegraph: The number of telegraph facilities
21. Post office: The number of post offices
22. Post box: The number of post boxes

23. Primary school: The number of primary schools
24. Guidance school: The number of guidance schools
25. High school: The number of high schools
26. Village name: The name of the villages
27. District: The name of the district of
28. Rural-district: The name of the rural district
29. Township: The name of the township
30. Province: The name of the province

(6) Contours

The contour line is mostly digitized from 1:25,000 topographic maps. It is 10 meters interval contour lines. However, in plains (near to Golestan Dam) 1:25000 maps weren't available. So, 1:50,000 maps have been utilized in this area. The image map of contour lines is shown as follow.

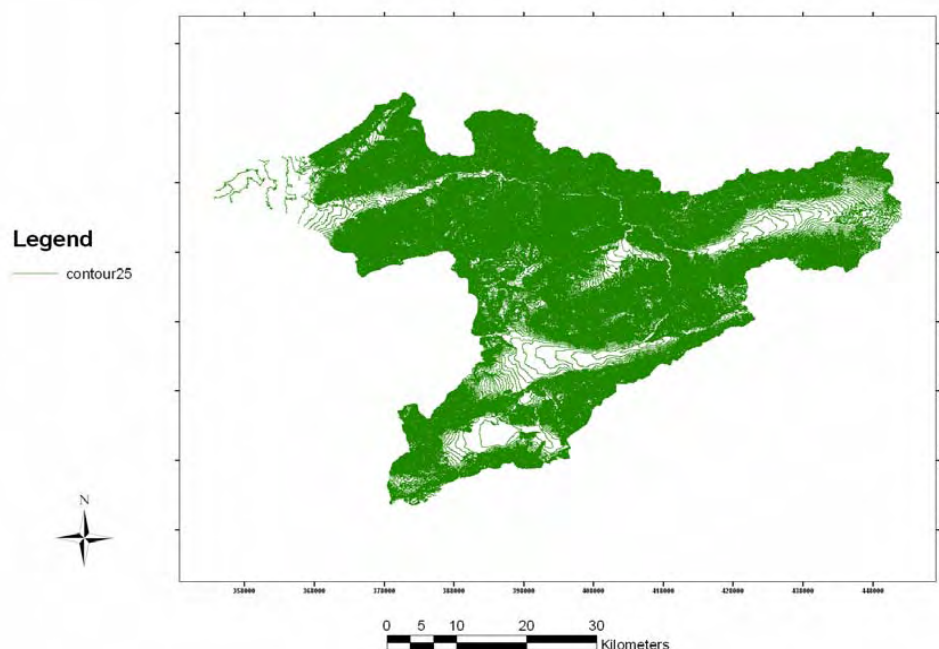


**Figure 2.23 Image Map of Contour Lines**

Using above contour line and elevation points, the DEM can be generated as follow.

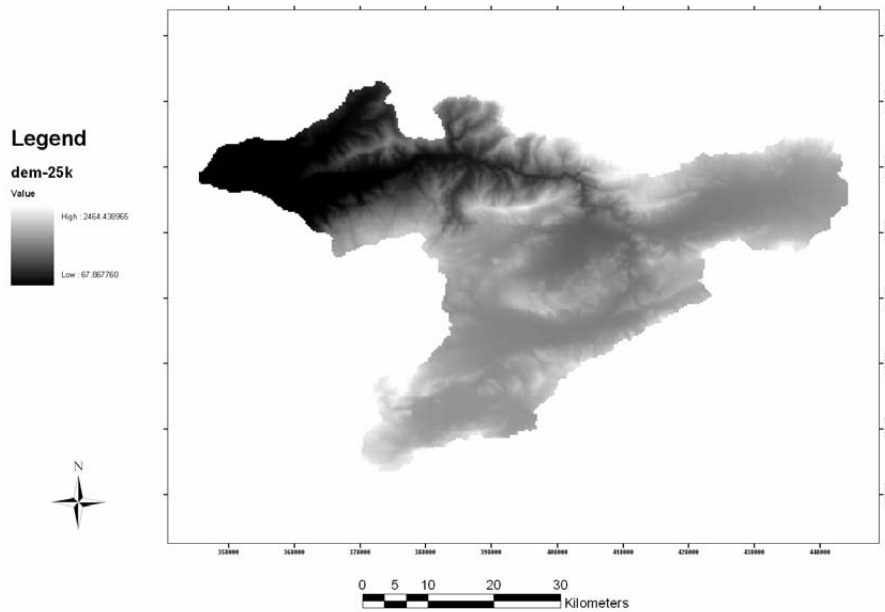


Figure 2.24 Image Map of DEM

## 2.4 GIS Database in 1:10,000 Scale

### 2.4.1 Topographic Map Data

Beside above GIS database mostly based on 1:25,000 scale topographic maps, JICA study team also established a big scale (1:10,000) GIS database based on Quick Bird satellite image in disaster area for analysis of food simulation and prepare of hazard map. The disaster area is a buffer zone along with river and its flat area which covered with 242 km<sup>2</sup>. This database includes detail land cover, detail contour line, river, road, bridge layers and so on. The layers except of land cover and contour were user 1:25,000 scale data as basis and updated by Quick Bird satellite image. Land cover was fully abstracted from Quick Bird, and contour line was generated from DEM and field survey in flat area.

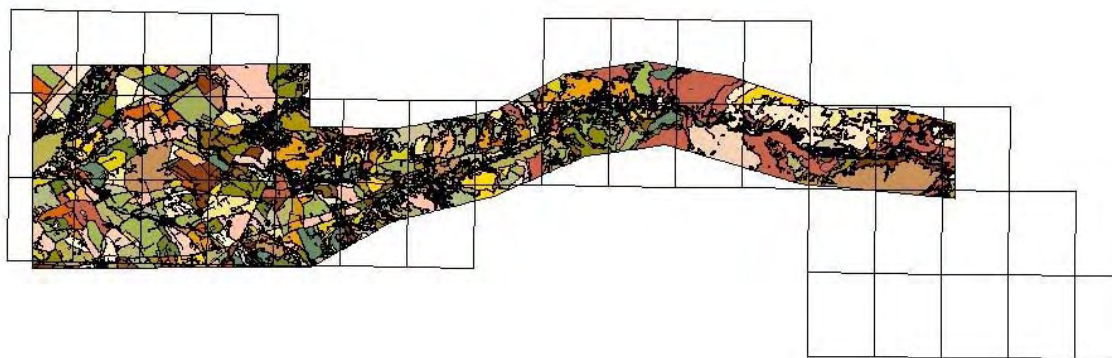


Figure 2.25 Image Map of 1:10,000 Scale Topographic Map Data

### 2.4.2 Land Cover

Land Cover was abstracted from Quick Bird satellite image. It includes 35 types of land cover from Agriculture, Major Building, Flooding, Forest, Range and so on. The design follows 1:10,000 USGS land cover map. The sample image is as follows.

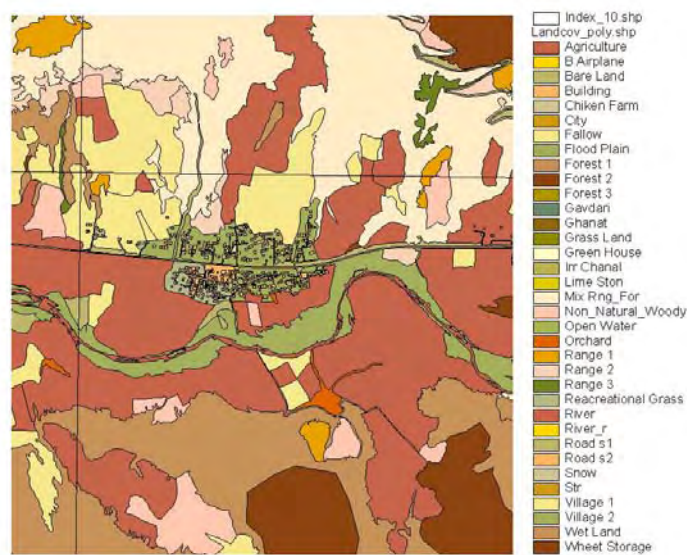


Figure 2.26 Image Map of 1:10,000 scale Land Cover

### 2.4.3 Contour Lines

The contour lines for 1:10,000 scale map was generated by DEM and field point survey in flat area. It is a 1 meter interval contour lines along with river and its flat area. It can be better use for food simulation analysis. The image map of the contour line is as follow.

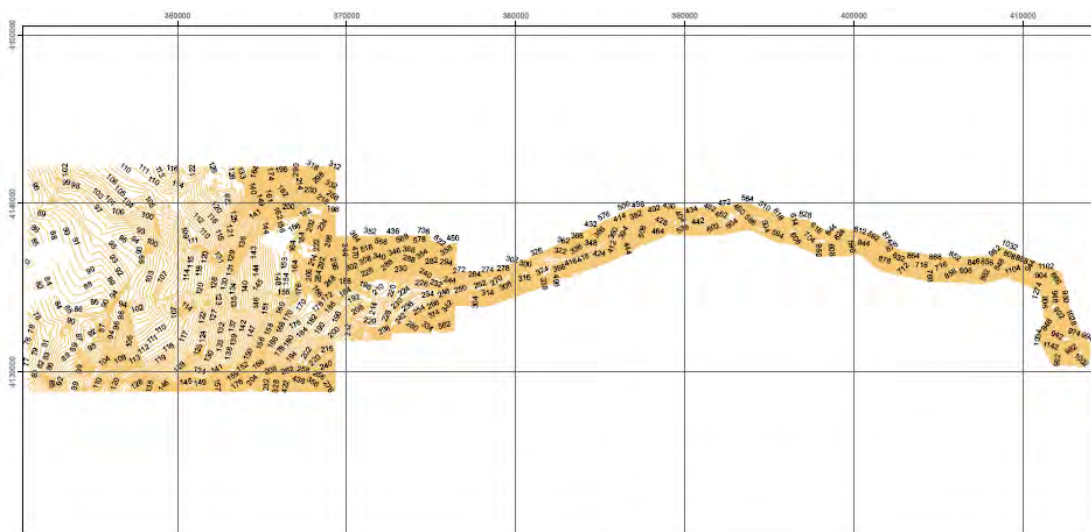


Figure 2.27 Image Map of 1:10,000 scale Contour Lines

### 2.5 GIS Data for Hazard Map Generation

In the disaster area, JICA study team also collected the information for floods in past years. As well as the analysis result for the future flood was also prepared into the GIS database for hazard map generation in next stage.

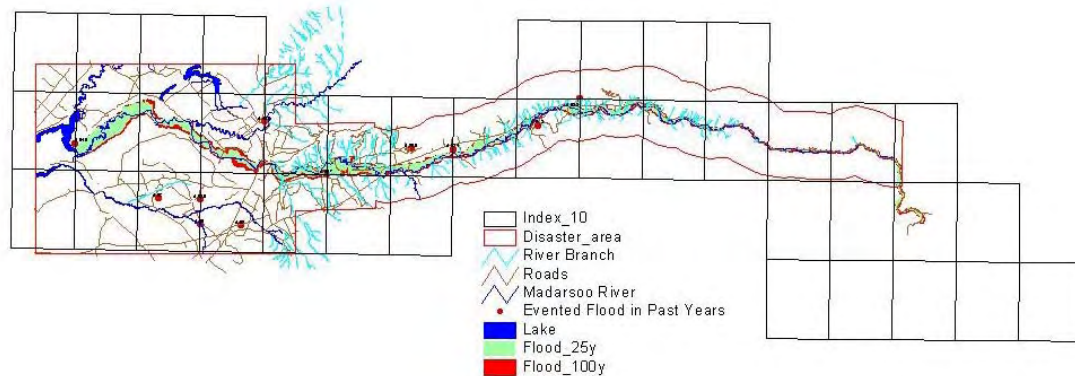


Figure 2.28 Image Map of Disaster Data

### 2.5.1 Flood Event in Past Years

Through the interview survey and flood information collection, JICA study team established a flood event database. It includes record and coordination of every flood event in the past years with a photos and videos album. The flood event map is shown in Figure 30 and the record of flood event is shown in following table. This information can be used in generating an education hazard map.

Table 2.8 Table of Flood Event in Past Years

ID	استان	Province	تاریخ وقوع رخ؟ ل	(Date)	PREVIOUS FLOOD	پس؟ ل قبل	EFFECTED AREA	ناح؟ تحت تاثیر؟
A 295	گلستان	golestan	08_11_1381	2001	Have	دارد	Gharesoo	قره سو
A 57	گلستان	golestan	28_7_1383	2003	Have	دارد	Atrak	اترک
A 540	گلستان	golestan	28_07_1383	2003	Have	دارد	Gorganrood	گرگان رود
A 696	گلستان	golestan	28_07_1383	2003	Have	دارد	Gorganrood	گرگان رود
A 55	گلستان	golestan	28_7_1383	2003	Have	دارد	Atrak	اترک
A 624	گلستان	golestan	15_05_1377	1997	Have	دارد	Gorganrood	گرگان رود
A 52	گلستان	golestan	28_7_1383	2003	Have	دارد	Atrak	اترک
A 538	گلستان	golestan	28_07_1383	2003	Have	دارد	Gorganrood	گرگان رود
A 518	گلستان	golestan	28_07_1383	2003	Have	دارد	Gorganrood	گرگان رود
A 405	گلستان	golestan	26_04_1382	2002	Have	دارد	Gorganrood	گرگان رود
A 547	گلستان	golestan	28_07_1383	2002	Have	دارد	Gorganrood	گرگان رود

ID	MainRiverName	نام رودخانه اصل	DAMAGE	Quantity	نوع خسارت	وحدت مقدار خسارت
A 295	Gharesoo	قره سو	FARMLAND	80 HECTAR	مزرعه	80 هکتار
A 57	Atrak	اترک	BRIDGE	1SET	پل	1 دهنه
A 540	Gorganrood	گرگان رود	DOMESTIC	15 KILLED	ح؟ وفات اهل	15 راس
A 696	Gorganrood	گرگان رود	FARMLAND	1HECTAR	مزرعه	1 هکتار
A 55	Atrak	اترک	FARMLAND	50 HECTAR	مزرعه	50 هکتار
A 624	Gorganrood	گرگان رود	FARMLAND	15 HECTAR	مزرعه	15 هکتار
A 52	Atrak	اترک	VEIHCLE	7 SET	وس؟ له نقل؟	7 دستگاہ
A 538	Gorganrood	گرگان رود	PERSON	6 PERSON, KILLED	انسان	6 نفر
A 518	SiyahJooy	گرگان رود				
A 405	Gorganrood	گرگان رود				
A 547	Gorganrood	گرگان رود				

### 2.5.2 Flood Simulation for 25 and 100 Years Flood

JICA study team used the above GIS database in flood simulation for 25 and 100 years. To overlay this simulation result with other GIS data layer, such as Quick Bird Image data, it is easy to know where will be easy to head the disaster in the future. Therefore people could be known where is the safe place and how to reach there. This information could be use in generating emergency hazard map.



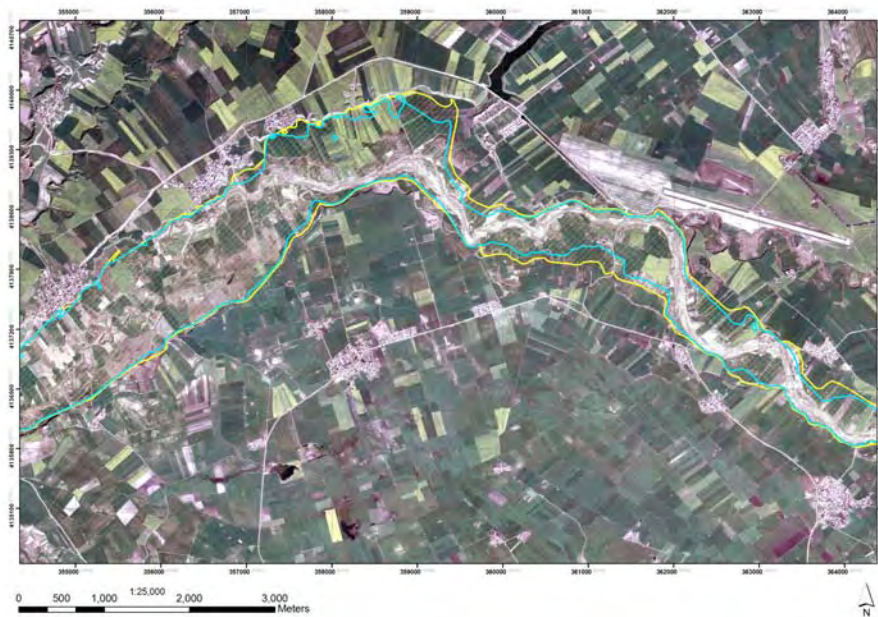


Figure 2.29 Image Map of Flood Simulation for 25 and 100 Years Flood

### 2.5.3 Landslide Disaster Data from Land Classification

Using Land Classification data in GIS database, the Landslide disaster area is easy to be abstracted. Then, to overlay this landslide data with other GIS data layer, such as slope, geology, land use, buildings and so on, people will easy to know where is landslide disaster's easy happening area, and where should be handled in high priority. Furthermore, flood control experts can use this information to reduce the damage from the flood.

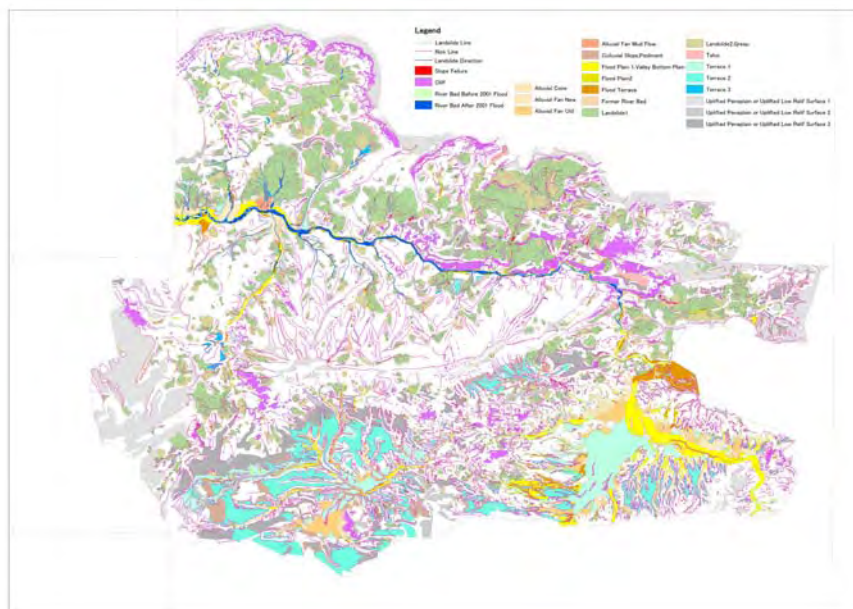


Figure 2.30 Image Map of Land Classification Data

---

---

*SUPPORTING REPORT I (MASTER PLAN)*

*PAPER XVII*

*Hydraulic Modeling*

---

---



**THE STUDY ON FLOOD AND DEBRIS FLOW  
IN THE CASPIAN COASTAL AREA  
FOCUSING ON THE FLOOD-HIT REGION  
IN GOLESTAN PROVINCE**

**SUPPORTING REPORT I (MASTER PLAN)**

**PAPER XVII HYDRAULIC MODELING SYSTEM**

**TABLE OF CONTENTS**

	Page
<b>CHAPTER 1 INTRODUCTION .....</b>	<b>XVII-1</b>
<b>CHAPTER 2 OBJECTIVES .....</b>	<b>XVII-2</b>
<b>CHAPTER 3 APPROACH.....</b>	<b>XVII-3</b>
<b>CHAPTER 4 OBTAIN AND REVIEW DATA (TASK 1).....</b>	<b>XVII-4</b>
4.1 Final DEM delivered by Iran Systems.....	XVII-4
4.1.1 Contours in the downstream end.....	XVII-4
4.1.2 Contours from Kalaleh to Agha Mish Bridge .....	XVII-5
4.1.3 Contours from Agha Mish to Besholy Bridge.....	XVII-6
4.1.4 Contours from Besholy to Golestan Fores .....	XVII-7
4.1.5 Comparison in Golestan Forest .....	XVII-8
4.1.6 Level discrepancies between the Iran Systems DEM and the MoE survey data .....	XVII-8
4.1.7 Comparison of the Madarsoo path with the 742 satellite image .....	XVII-9
4.1.8 Detailed comparison in the upstream end .....	XVII-10
4.1.9 Summary .....	XVII-11
4.2 Field trip 14 August 2005 .....	XVII-11
4.2.1 Kalaleh Road .....	XVII-12
4.2.2 Kalaleh Bridge.....	XVII-13
4.2.3 Road from Kalaleh Bridge to Ajen Ghare Khajeh Bridge .....	XVII-13
4.2.4 Ajen Ghare Khajeh Bridge .....	XVII-13
4.2.5 Gravel road down to Tangrah Road from Ajen Ghare Khajeh Bridge .....	XVII-13

4.2.6	Tangrah Road .....	XVII-13
4.2.7	Road in Golestan Forest .....	XVII-13
4.2.8	Golestan Dam .....	XVII-13
4.2.9	Downstream end of Madarsoo .....	XVII-14
4.3	Satellite imagery .....	XVII-15
4.4	Mosaic DEM created from resampled 85 m DEM and Iran Systems DEM .....	XVII-16
4.4.1	Augmentation of mosaic DEM with MoE survey cross-sections.....	XVII-16
4.4.2	How to “burn” the Madarsoo channel into the DEM .....	XVII-17
4.5	Summary.....	XVII-18
<b>CHAPTER 5</b>	<b>HYDROLOGY (TASK 3) .....</b>	<b>XVII-20</b>
5.1	Extraction of boundary conditions for the single branch MIKE 11 model .....	XVII-20
5.1.1	Translation to a different network .....	XVII-21
<b>CHAPTER 6</b>	<b>DEBRIS FLOW (TASK 4).....</b>	<b>XVII-22</b>
6.1	Calculation of the debris yield using the Los Angeles District Debris Method .....	XVII-22
6.2	Distribution in time of the debris flow.....	XVII-24
6.3	Particle size distribution of the debris flow .....	XVII-25
6.4	Timing of the debris flow and the Madarsoo hydrograph .....	XVII-25
6.4.1	Longitudinal distribution of the debris .....	XVII-26
<b>CHAPTER 7</b>	<b>MIKE 11 HD+ST MODEL (TASK 5).....</b>	<b>XVII-29</b>
7.1	Bridges.....	XVII-29
7.1.1	Transformation to a different network and cross-sections.....	XVII-31
7.1.2	Bridges of Golestan Forest .....	XVII-31
7.1.3	14 Metry Bridge .....	XVII-31
7.1.4	Backwater calculation for 1600 m <sup>3</sup> /s .....	XVII-32
7.2	MIKE 11 model based on “mosaic” DEM .....	XVII-34
7.3	Bridges in the “mosaic” network .....	XVII-35
7.4	Backwater calculations in the mosaic MIKE 11 model.....	XVII-37
7.5	Inclusion of debris flow in mosaic model.....	XVII-39
7.6	MIKE 11 morphological model parameters .....	XVII-39

7.7	Model based on Final Iran Systems DEM .....	XVII-39
<b>CHAPTER 8</b>	<b>MODEL APPLICATIONS .....</b>	<b>XVII-41</b>
8.1	Results for overall MIKE 11 HD model .....	XVII-41
8.1.1	Animation of the 100 year flood .....	XVII-41
8.1.2	Flood maps .....	XVII-44
8.1.3	Comparison with flood markers for the 2001 flood ...	XVII-44
8.1.4	Road overtopping between 14 Metry Bridge and Tangrah.....	XVII-45
8.1.5	14 Metry Bridge .....	XVII-46
8.1.6	Appropriate simulation period for MIKE 11 HD+ST model .....	XVII-46
8.2	Results for local MIKE 11 HD+ST model .....	XVII-47
8.2.1	Temporal development of the debris dams .....	XVII-47
8.2.2	Bed level and water level profiles .....	XVII-47
8.2.3	The surging effect.....	XVII-49
8.2.4	Flood maps and flood extend .....	XVII-50
<b>CHAPTER 9</b>	<b>SUMMARY OF ACTIVITIES CARRIED OUT 6 AUGUST -17 SEPTEMBER 2005.....</b>	<b>XVII-52</b>
<b>CHAPTER 10</b>	<b>CONCLUSIONS .....</b>	<b>XVII-57</b>
<b>REFERENCES</b>	<b>.....</b>	<b>XVII-60</b>
<b>APPENDIX A</b>	<b>FLOOD MAPS 100 YEAR EVENT .....</b>	<b>XVII-61</b>
<b>APPENDIX B</b>	<b>ROAD OVERTOPPING 14 METRY BRIDGE TO TANGRAH .....</b>	<b>XVII-69</b>

### **LIST OF TABLES**

Table 6.1	Calculated debris yields (2001 flood) for the selected debris flow prone tributaries .....	XVII-23
Table 6.2	Calculated debris yield for each of the selected debris prone tributaries for the five different events (2001, 2005, 25, 50, 100 year).....	XVII-24
Table 7.1	The 19 bridges to be included in the hydraulic model; road elevations and culvert inverts estimated from crosssection survey data .....	XVII-30
Table 7.2	Geometries for each of the culverts and weirs, estimated from the MoE cross-section survey data. The three first columns are for the culvert, while the two last columns are for the weir. For “Geometry” one number indicates a diameter, while two numbers are width and height, and for 14 Metry Bridge the culvert is special to represent the arch opening, which is described in detail in asub-section.....	XVII-30
Table 7.3	Bridge locations in network based on MoE data and Ira Systems DEM.....	XVII-36
Table 7.4	Culvert and road elevations for the bridges estimated from the Mosaic cross-sections. The “Difference” is to the MoE section estimated elevations .....	XVII-36
Table 8.1	Calculation of water depth above 14 Metry Bridge for 25, 50 and 100 year peak discharge .....	XVII-46

### **LIST OF FIGURES**

Figure 4.1	Contour lines for the DEM in the downstream end. It is noted that Iran Systems came later with an updated DEM where the downstream end was vastly improved.....	XVII-5
Figure 4.2	Contour lines from Iran Systems from Kalaleh Bridge to Agha Mish Bridge. The Madarsoo branch according to the MoE survey data is shown in blue, while the red line shows the branch following the contour lines .....	XVII-5
Figure 4.3	Contours from Agha Mish to Besholy; here we have started adding Tangrah Road, why will be apparent later .....	XVII-6

Figure 4.4	Contours from Besholy to Golestan Forest. Here we have added the survey points from the field trip conducted on 14 August 2005 by the DHI expert.....	XVII-7
Figure 4.5	Close-up of the area where the DEM says the Madarsoo should cross Tangrah Road, and where the MoE data says the river runs into the hills.....	XVII-7
Figure 4.6	Comparison between the Iran Systems DEM and the MoE path of the river in Golestan Forest.....	XVII-8
Figure 4.7	Elevation difference between the Iran Systems DEM and the MoE survey cross-sections (converted to DEM).....	XVII-8
Figure 4.8	Madarsoo branch in Golestan Forest from three sources 742 satellite image, MoE survey data and Iran Systems DEM. The two circles indicate areas with major discrepancies.....	XVII-9
Figure 4.9	Detail of the Madarsoo branch from the 742 satellite image just upstream of Tangrah.....	XVII-9
Figure 4.10	Detail of the Madarsoo branch from the 742 satellite in Golestan Forest.....	XVII-10
Figure 4.11	Detail of the Madarsoo branch from the 742 satellite in the upstream end of Golestan Forest (8 km downstream of Dasht).....	XVII-10
Figure 4.12	Iran Systems DEM and contour lines. Left Contour lines corresponding to the DEM, and Right ..... Contour lines generated from the MoE cross-section survey data.....	XVII-11
Figure 4.13	Field trip conducted on 14 August 2005 with 82 GPS points.....	XVII-12
Figure 4.14	The two elevations obtained in the downstream end of Madarsoo. The GPS locations match the surveyed river very well.....	XVII-14
Figure 4.15	The downstream GPS water level with +/- 10 m range, the D6174 survey cross-section at the same location, and DEM sections extracted along the survey line for the cross-section.....	XVII-14
Figure 4.16	The downstream GPS water level with +/- 10 m range, the D6050 survey cross-section at the same location, and DEM sections extracted along the survey line for the cross-section.....	XVII-15
Figure 4.17	Quick Bird satellite image (pixel size 60 cm).....	XVII-16
Figure 4.18	742 satellite image (pixel size 28.5 m).....	XVII-16
Figure 4.19	Mosaic DEM created by the resampled 85 m DEM (left of the black line) and the Iran Systems DEM (to the right of the black line)	XVII-16



Figure 4.20	Iran Systems DEM and contour lines created from the MoE survey cross-sections in Golestan Forest about 15 km from the upstream boundary.....	XVII-17
Figure 5.1	Locations of the boundary conditions extracted from the MIKE 11/SHE model. Each boundary condition has a location and an associated discharge time-series for each of the five scenarios .....	XVII-20
Figure 6.1	The eleven locations with debris flow observed during the 2001 flood (red circles), and the corresponding tributaries, along the left bank F102B, F102, F101B/F101A/Kondoskooh and along the right bank F03, F02, F01, T01, T03, T04, T06 and T07.....	XVII-22
Figure 6.2	Debris yield for each drainage for the five scenarios (2001, 2005, 25, 50, 100 year).....	XVII-24
Figure 6.3	Debris flow rates calculated with $a=0.8$ for the 2001 flood .....	XVII-25
Figure 6.4	Depth-Width curves for the crosssections that the debris prone tributaries enter in the Madarsoo network (Iran Systems version).	XVII-27
Figure 6.5	Calculated height of the debris deposit for each tributary for all five scenarios by assuming a triangular shape.....	XVII-27
Figure 7.1	The 19 Bridges in the MIKE 11 model. The Ajen Ghare Khajeh Bridge is new compared to the list data from February .....	XVII-29
Figure 7.2	Level-width curves for 14 Metry Bridge (culvert and weir) .....	XVII-31
Figure 7.3	Backwater calculation at 14 Metry (and 7 Culverts) Bridge. The inverts (culvert and road) are shown for each bridge. It is seen that 14 Metry backs the water up more than 1 km .....	XVII-32
Figure 7.4	Q-H relations for the two structures (culvert and weir) comprising 14 Metry Bridge .....	XVII-33
Figure 7.5	Backwater curves for all 19 bridges calculated for a constant discharge of 1600 m <sup>3</sup> /s. ....	XVII-33
Figure 7.6	Backwater curves for the bridges in Golestan Forest.....	XVII-33
Figure 7.7	Backwater curves for the bridges downstream of Golestan Forest	XVII-34
Figure 7.8	Mosaic DEM with MIKE 11 network and MIKE 11 cross-sections. The bridge locations are only for reference; they are not included in this model. The bridges will be included if we deem that this is the MIKE 11 model we will use, but it requires changes to the chainages and inverts of the bridges .....	XVII-34

Figure 7.9	Bridge backwater (water level with bridges minus water level without bridges) calculated with “Mosaic” MIKE 11 model with a Manning $n=0.04 \text{ s/m}^{1/3}$ .....	XVII-37
Figure 7.10	Bridge backwater (water level with bridges minus water level without bridges) calculated with “Mosaic” MIKE 11 model with a Manning $n=0.04 \text{ s/m}^{1/3}$ .....	XVII-37
Figure 7.11	Bridge backwater (water level with bridges minus water level without bridges) calculated with “Mosaic” MIKE 11 model with a Manning $n=0.04 \text{ s/m}^{1/3}$ , and modified level-width curves that match the cross-sections .....	XVII-38
Figure 7.12	Bridge backwater (water level with bridges minus water level without Bridges) calculated with “Mosaic” MIKE 11 model with a Manning $n=0.20 \text{ s/m}^{1/3}$ , and modified level-width curves that match the cross-sections .....	XVII-38
Figure 7.13	The eleven debris flow tributaries and the chainages in the Madarsoo network to which the debris flow timeseries are added .....	XVII-39
Figure 7.14	Downstream end of the Iran Systems DEM received on 12 September 2005. The DEM is vastly improved over the DEM received in August in which the terrace was not represented .....	XVII-40
Figure 8.1	Flood maps (100 year event) from the animation with the 742 satellite image .....	XVII-43
Figure 8.2	Flood maps based on simulated maximum flood levels, from top 25 years, 50 years and 100 years return period .....	XVII-44
Figure 8.3	The seven (10 km long starting from 360 km Easting UTM-40) areas where the flood maps are shown in Appendix A .....	XVII-44
Figure 8.4	Comparison between the 50 years flood extend and flood markers for the 2001 flood.....	XVII-44
Figure 8.5	Overtopping of Tangrah Road between 14 Metry Bridge and Tangrah determined from the 100 year flood map and the location of Tangrah road (from 1:25,000 map confirmed with GPS points). Four locations (1-4) are identified from this map .....	XVII-45
Figure 8.6	Upstream discharge (boundary condition) and downstream discharge (simulated) from the MIKE 11 HD model for each of the scenarios. Note that each scenario starts on 10 August, except the 2005 flood that starts 9 August. For better representation we moved the 2005 flood to start on 10 August in this figure. The simulation period to be used for	

	the HD+ST models is selected as 10 August 22:00 to 12 August 00:00 (9-11 August for 2005 flood) .....	XVII-46
Figure 8.7	Temporal development of the bed level minus the initial bed level for all the debris dams shown along with the water inflow.....	XVII-47
Figure 8.8	Profiles of the maximum water level (with and without debris) and maximum bed level (with debris) for the debris flow simulation with the 100 year event, upstream part of the local debris model .....	XVII-48
Figure 8.9	Profiles of the maximum water level (with and without debris) and maximum bed level (with debris) for the debris flow simulation with the 100 year event, downstream part of the local debris model .....	XVII-48
Figure 8.10	Difference in maximum bed and water level caused by the presence of debris flow (100 year event) .....	XVII-48
Figure 8.11	Temporal variation of the downstream discharge in the local debris model with and without debris flow included .....	XVII-49
Figure 8.12	The longitudinal variation in the difference in peak discharge (with debris minus without debris) down through the local model .....	XVII-49
Figure 8.13	Flood map for the local model (100 year flood, maximum flood level) with debris flow included.....	XVII-50
Figure 8.14	Comparison map (maximum depth with debris minus maximum depth without debris) for the 100 year flood.....	XVII-50
Figure 8.15	Flood extend with and without debris flow for the 100 year flood	XVII-51

## **CHAPTER 1 INTRODUCTION**

This report describes the activities carried out by the DHI expert in the period 6 August - 16 September 2005. The following activities were planned:

- Receive and quality check the final DEM from Iran Systems
- Prepare data (geometry and inverts) for all bridges crossing the Madarsoo in the model reach.
- Construct MIKE 11 ST model based on the Iran Systems DEM and MoE cross-sections if possible.
- Implement the bridges in the model to account for backwater.
- Process hydrology model results into time-series and water point sources for the single branch Madarsoo model we are to use in the MIKE 11 ST and flood mapping model.
- Identify debris prone tributaries and calculate the debris flow using a method from the literature. Calculate time-series of the debris flow and include as sediment point sources in MIKE 11 ST.
- Perform production runs with the MIKE 11 ST model
- Prepare flood maps and flood animations based on the MIKE 11 ST results

## **CHAPTER 2      OBJECTIVES**

The objectives of the DHI model study are to:

- ❑ Construct a MIKE 11 hydraulic model that can dynamically simulate flashfloods taking place in the Madarsoo River from Dasht village to Golestan reservoir.
- ❑ Apply the hydraulic model to produce flood maps for the 25 year, 50 year and 100 year flood events in the Madarsoo River from Dasht village to Golestan reservoir.
- ❑ Quantify the hydraulic impact (extend of flood and flood depth) of debris flow in relevant tributaries along the Madarsoo River.

## **CHAPTER 3    APPROACH**

To meet the objectives, we employ the following approach:

- A MIKE 11 model network is defined for routing the floodwaters down through the Madarsoo. This network should represent the path of the floodwaters rather than the path of the river. In addition the DEM is not consistent with the available Quick Bird satellite images, so we chose to define the river network to be consistent with the DEM.
- Cross-sections for the MIKE 11 model were drawn on top of the DEM using the river network and an extreme flood extent calculated with a 2D model. Survey cross-sections from MoE have to be omitted because the elevations are incompatible with the elevations in the DEM. The MIKE 11 model is hence purely based on the DEM.
- Boundary conditions for the MIKE 11 hydraulic model have been calculated with a hydrological model (MIKE SHE) using rainfall and topography as well as routing through a MIKE 11 network. Boundary conditions were produced for the 25 year, 50 year, 100 year, 2001 and 2005 floods.
- Calibration is very difficult for this model because it has to be used for extreme flood conditions where there is no water level data because the gauges are destroyed during these events. Calibration is therefore based on estimated values for the Manning n in a river and floodplain like this one.
- Debris flow has been handled by using empirical formulas for the debris yield combined with assumptions about the distribution in time of the debris flow, resulting in time-series for the debris inflow, which are added as sediment point sources at the junctions with the debris carrying tributaries. The MIKE 11 model is then extended to include sediment transport, which results in the formation and erosion of debris deposits that impact the hydraulics. The impact of debris flow is quantified with this approach.
- Flood maps are generated in MIKE 11 GIS, which translates the 1D hydraulic model into 2D maps of the floods. Flood maps are delivered for the 25 year, 50 year and 100 year floods, and local flood maps in the debris prone reach of the Madarsoo River are delivered along with comparison maps to quantify the hydraulic impact of debris flow.

## CHAPTER 4 OBTAIN AND REVIEW DATA (TASK 1)

Flood mapping is a delicate procedure in which inconsistencies in the data behind the mapping will be shown very clearly in the maps:

- Elevation inconsistencies in the DEM and cross-sections will give rise to flood maps in which the river is either transformed to an “aqueduct” or “groundwater”. This will be manifested in the flood maps as either complete absence of flooding (groundwater; water level below DEM) or exaggerated flooding (water level too high compared to DEM). There is no escaping these deficiencies if one uses inconsistent data.
- Inconsistencies can also result in the flood map moving away from the river.

Both of the above can be demonstrated with the present lack of data consistency. In fact there are literally no consistent elevation sources available.

A mathematical model is no better than the data that lies behind the model. A mathematical model does not possess magic powers to correct for errors in the data; it is no better than the data quality. In modeling we often express this as:

Garbage in = garbage out

Regarding inconsistencies in the data, if there are two elevations given by two different data source, then one of the must be wrong. Of course there is no guarantee that any of them is correct; they might both be wrong, but they cannot both be correct.

### 4.1 Final DEM delivered by Iran Systems

According to Iran Systems the DEM that has been used by in the hydrological modeling was based on satellite images from the space shuttle. This DEM was analyzed by the DHI expert (not reported here), and it was a preliminary DEM that Iran Systems think is not good enough.

A new and supposedly final DEM was received on Monday 22 August 2005, while preliminary contours for this DEM were received two days before on 20 August. Revised contour lines (some editing done) were received along with the DEM on Monday 22 August.

In the following sub-sections we will look in detail at the Iran Systems contours, the MoE data and other GIS shapes that we have available. It is tedious work and tedious to read, but it is necessary for the consultant to point out the major data discrepancies that are going to put a limit on the quality of the output.

It is noted that a modified and much improved DEM was received from Iran Systems on 12 September 2005. However, there was no time to alter the whole report, so it is kept as it was written before the final DEM was received.

#### 4.1.1 Contours in the downstream end

The contour lines for this DEM looked very suspicious in the downstream end, see Figure 4.1. Somehow the contours looked extraordinarily smooth considering that there should be dense point data behind it.

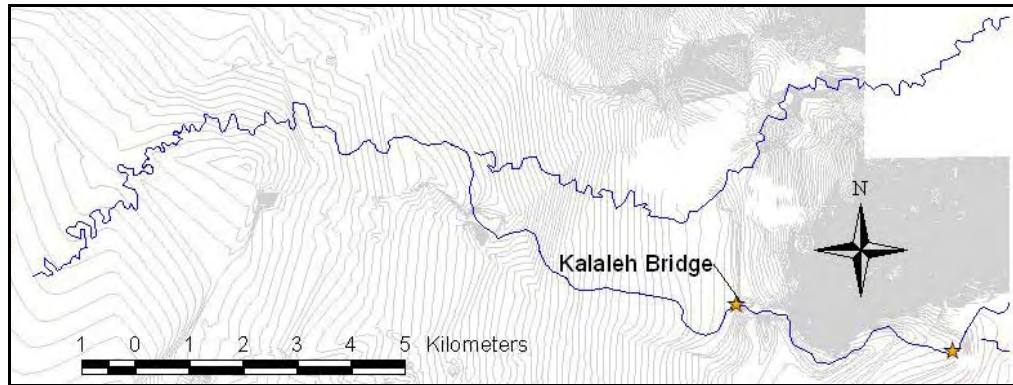


**Figure 4.1** Contour lines for the DEM in the downstream end. It is noted that Iran Systems came later with an updated DEM where the downstream end was vastly improved.

The crucial terrace and incised floodplain are non-existent in these contours. Apparently the DEM has been based on survey data in the downstream end, a procedure that can in principle function, but the data density has to be very high to produce 2 m contours, as Iran Systems have done. Of course one can produce 2 m contours by just interpolating; one can produce 1 cm contours from a data source, but such contours are not worth anything if the data source does not have the accuracy to allow such contours.

According to Iran Systems no survey data has been collected in the incised floodplain, which would explain the straight contour lines that clearly do not reflect the incised floodplain.

The JICA team has requested the survey point data from Iran Systems in order to check whether the DEM in any way can be salvaged for use in the project, or whether it should be discarded completely. It is doubtful that Iran Systems will be able to measure enough spot elevations to produce a reliable DEM in the downstream end. At this point it seems that the old 85 m grid DEM is better with its 85 m grid spacing than the apparently 200 m grid spacing that Iran Systems can measure spot elevations with.

#### 4.1.2 Contours from Kalaleh to Agha Mish Bridge

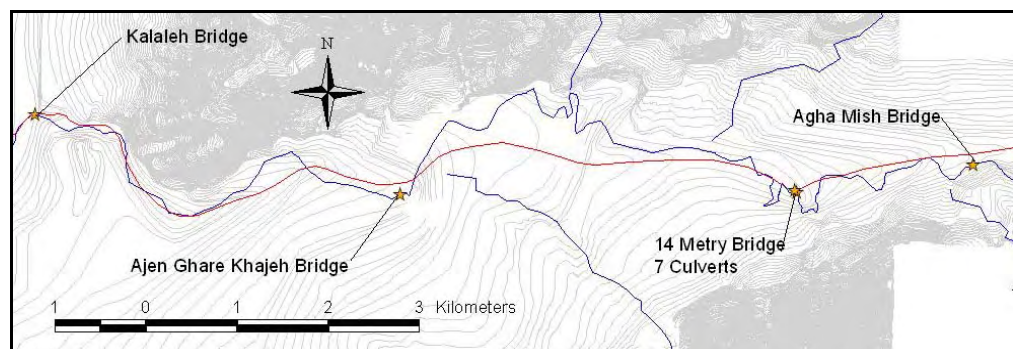


**Figure 4.2** Contour lines from Iran Systems from Kalaleh Bridge to Agha Mish Bridge. The Madarsoo branch according to the MoE survey data is shown in blue, while the red line shows the branch following the contour lines.

The contour lines from Kalaleh Bridge to Agha Mish Bridge are shown in Figure 4.2. Again these 2 m contours seem very smooth considering that they are 2 m contours. Our comments:

- For the upstream approach towards Kalaleh Bridge we know that the river channel is incised, which is at least to some extent reflected in the Iran Systems contour lines at this location.



- ❑ There are discrepancies between the path of the river in the DEM and in the survey data. In this area these discrepancies are less severe than we will see further upstream. For the largest discrepancy in the middle there is a village lying right where Madarsoo will go through when we apply this DEM. There is nothing we can do about this; it will have to be accepted.
- ❑ The meandering pattern of the river is not present at all in the DEM. This could indicate that the incised river channel is not resolved, though this seems to be the case at Kalaleh Bridge.

Even though the discrepancies in this area between the path of the river in the DEM and in the MoE survey data is less severe than we will find further upstream, it still means it will be very difficult to combine the MoE data and the Iran Systems data.

#### 4.1.3 Contours from Agha Mish to Besholy Bridge

In the Agha Mish to Besholy reach, see Figure 4.3, the river valley becomes narrower and the side slope increases. We make the following comments:

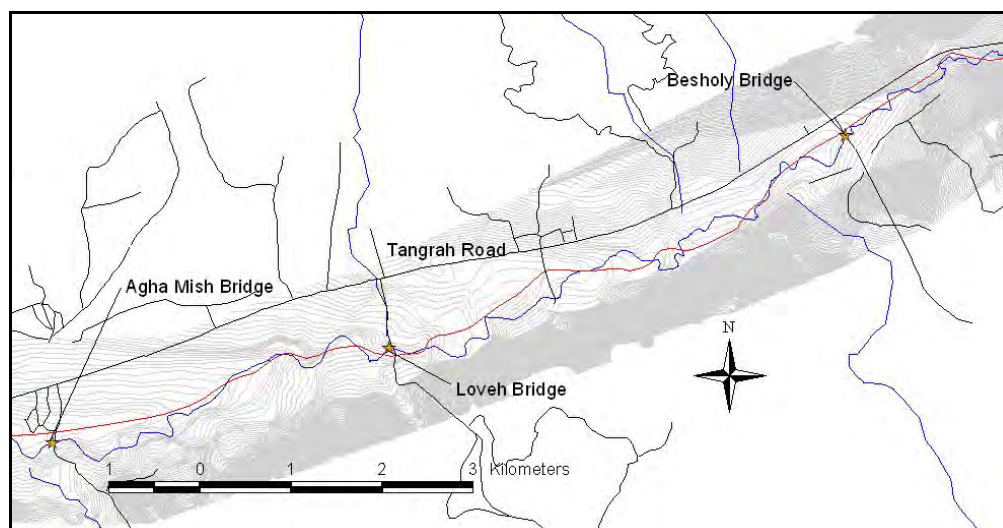


**Figure 4.3** Contours from Agha Mish to Besholy; here we have started adding Tangrah Road, why will be apparent later.

- ❑ There are several discrepancies between the river location in the MoE data and in the Iran Systems contour lines. In this area such discrepancies become much more severe because of the steeper valley. When looking at the MoE path the river clearly takes many sidesteps into high ground, which makes it very difficult to combine the MoE data and the Iran Systems DEM.
- ❑ Again the meandering pattern is not reflected in the DEM.

#### 4.1.4 Contours from Besholy to Golestan Forest

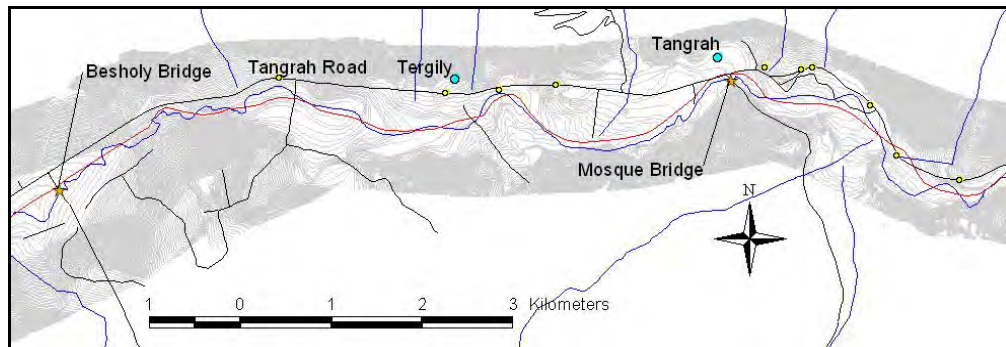


**Figure 4.4** Contours from Besholy to Golestan Forest. Here we have added the survey points from the field trip conducted on 14 August 2005 by the DHI expert.

The contours from Besholy to Golestan Forest are shown in Figure 4.4. Our comments are the same as for the Agha Mish to Besholy reach, but here we can add that the river crosses Tangrah Road in the upstream part of this reach (to the right in the figure). We believe the location of the road is accurate, which is confirmed when comparing with the survey points.

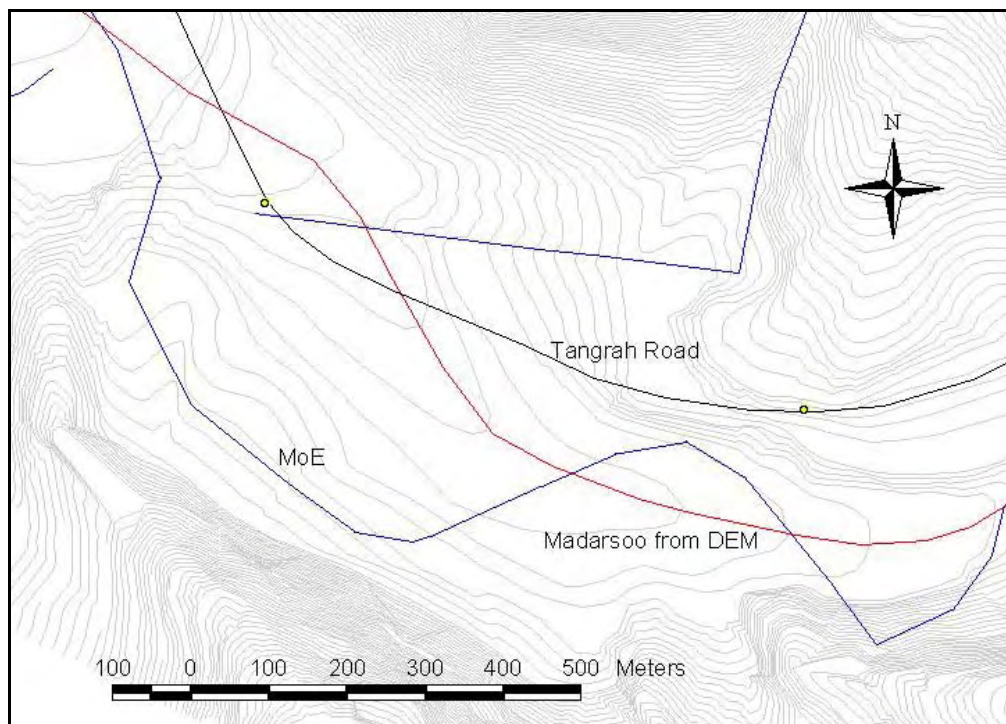


**Figure 4.5** Close-up of the area where the DEM says the Madarsoo should cross Tangrah Road, and where the MoE data says the river runs into the hills.

To further demonstrate the magnitude of this discrepancy the area in question is shown in detail in Figure 4.5. The comparison between the MoE survey data and the Iran Systems contours suggest that the river increases its elevation about 10 m, as it runs into the hill left of the Madarsoo, and it is even worse to the right in the picture where the river location according to the MoE data is right on the very steep side slope of the valley.

It is worth noting that the meandering pattern that the MoE data is shown does fit at all into the DEM. This is perhaps the largest discrepancy; we may have that the river does not always

fit, but how can MoE have measured this meandering pattern, when there is no room according to Iran Systems.

It is clear at this point that the Quick Bird images will be very important as an alternative source for figuring out the path of the Madarsoo River.

#### 4.1.5 Comparison in Golestan Forest

In Golestan Forest we switch to comparing with the DEM (corresponding to the contours) because the contours become too concentrated on the slopes.

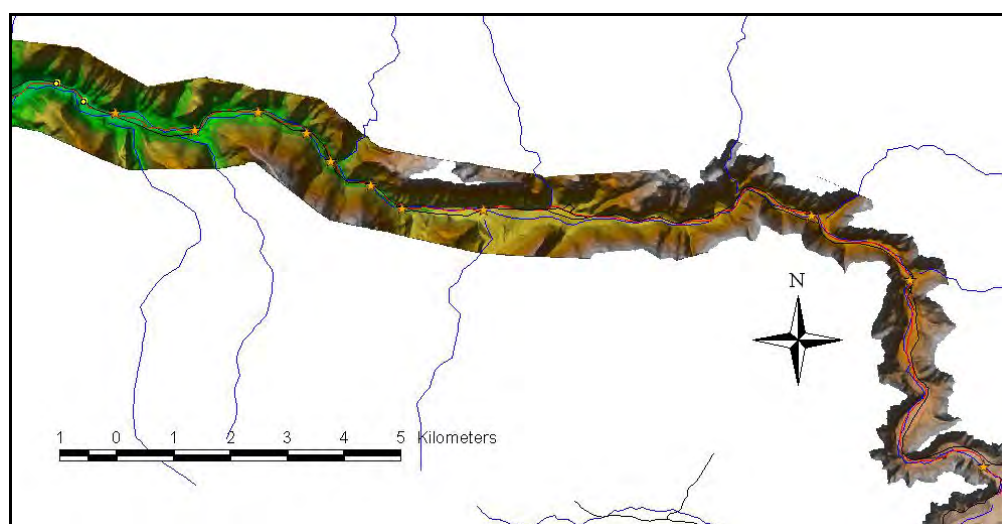


**Figure 4.6 Comparison between the Iran Systems DEM and the MoE path of the river in Golestan Forest.**

The characters of the discrepancies are the same, as for the areas further downstream.

#### 4.1.6 Level discrepancies between the Iran Systems DEM and the MoE survey data

As we have seen earlier, there are major discrepancies between the elevations in the MoE survey cross-sections and each DEM.

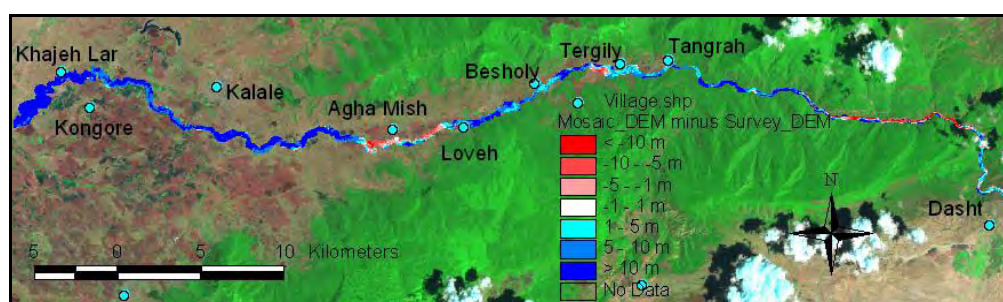
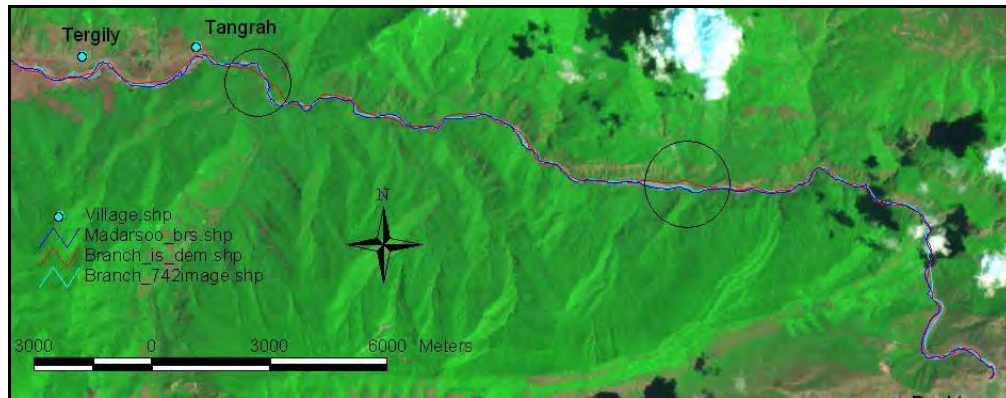


**Figure 4.7 Elevation difference between the Iran Systems DEM and the MoE survey cross-sections (converted to DEM).**

Figure 4.7 shows the level differences between the Mosaic DEM and a DEM created from the MoE survey cross-sections. The elevations often differ by more than 10 m (and there is only one correct elevation), which makes it impossible to combine these two data sets as they are in a hydraulic model.

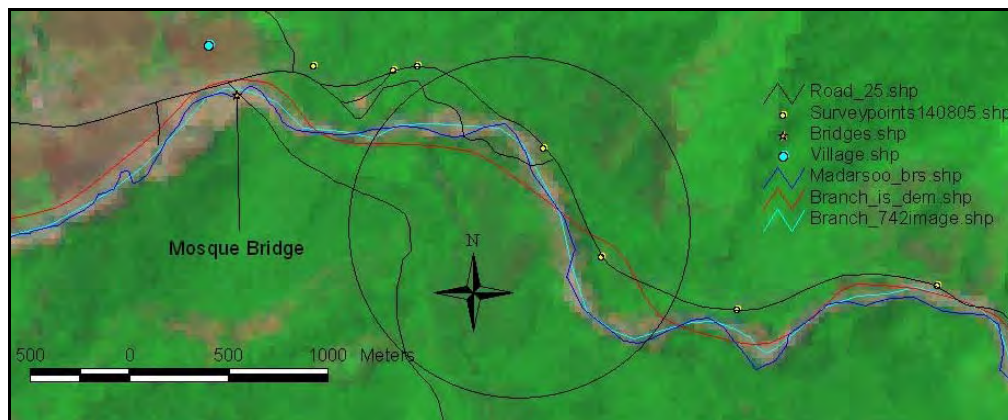
#### 4.1.7 Comparison of the Madarsoo path with the 742 satellite image

The path of the Madarsoo can be obtained from one more source, namely the 742 satellite image with a pixel size around 28.5 m. When the Quick Bird images become available in the upstream end, we will repeat this exercise and find the path according to the Quick Bird images (pixel size 60 cm).



**Figure 4.8 Madarsoo branch in Golestan Forest from three sources: 742 satellite image, MoE survey data and Iran Systems DEM. The two circles indicate areas with major discrepancies.**

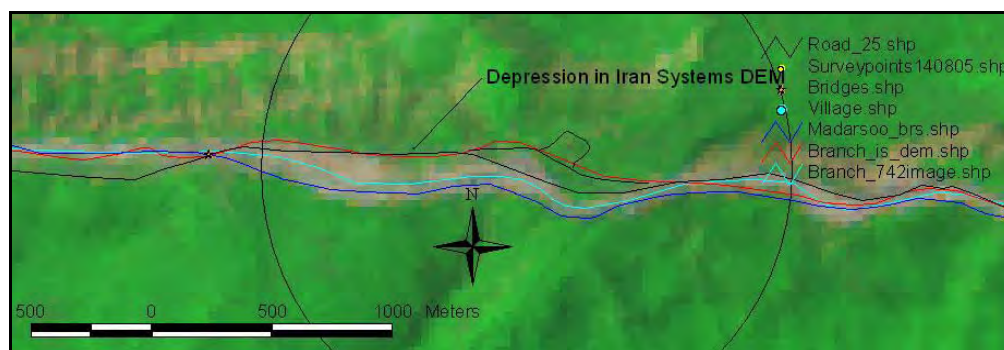
Figure 4.8 shows the path digitized from the 742 satellite image along with the path from the MoE survey data and the path from the Iran Systems DEM. The path is easily recognized in Golestan Forest, but become more difficult further downstream (Quick Bird better), so we focus on the Madarsoo location in Golestan Forest.



**Figure 4.9 Detail of the Madarsoo branch from the 742 satellite image just upstream of Tangrah.**

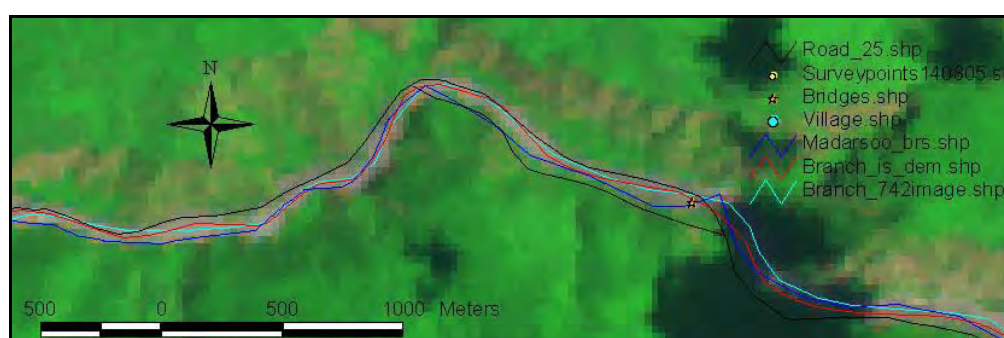
In the following we focus on the two areas marked with circles.

Figure 4.9 shows the discrepancy just upstream of Tangrah. The Golestan Forest road and the GPS survey points collected on the road on 14 August 2005 are shown as well for reference (the road location matches in the shape file and in the GPS points). The figure strongly suggests that the MoE survey data is fairly accurate (but still with discrepancies), while the Iran Systems DEM is very different from what the satellite image would imply.



**Figure 4.10** Detail of the Madarsoo branch from the 742 satellite in Golestan Forest.

Further upstream we have the strange depression that the Iran Systems DEM has to the right of Madarsoo, see Figure 4.10. Again the path of the Madarsoo is fairly well matched in the MoE data and in the 742 satellite image, but very off in the Iran Systems DEM.



**Figure 4.11** Detail of the Madarsoo branch from the 742 satellite in the upstream end of Golestan Forest (8 km downstream of Dasht).

It should be said that there are a few places where the Iran Systems DEM actually matches better with the satellite image than the MoE survey data. One such place is the sharp bend further upstream (Figure 4.11) where the MoE data ventures into the hills, while the Iran Systems DEM actually matches well with the satellite image. However, in general it is the Iran Systems DEM that has the largest discrepancies.

Unfortunately we have no choice but to use this DEM and the result in terms of flood mapping is easily predicted; the Madarsoo will flood where the Iran Systems DEM says the low elevations are, which is often contradictory to the 742 satellite image. We do not know yet what the Quick Bird image will give for the Madarsoo path.

#### 4.1.8 Detailed comparison in the upstream end

Here we look at the shape of the topography in the upstream end. We do this by comparing the Iran Systems DEM and contours to contours created from the MoE survey cross-sections. The purpose is to demonstrate that the Iran Systems DEM does not properly represent the incision of the Madarsoo into the valley. In many areas it is as if the incised channel is absent in the data behind the Iran Systems DEM.

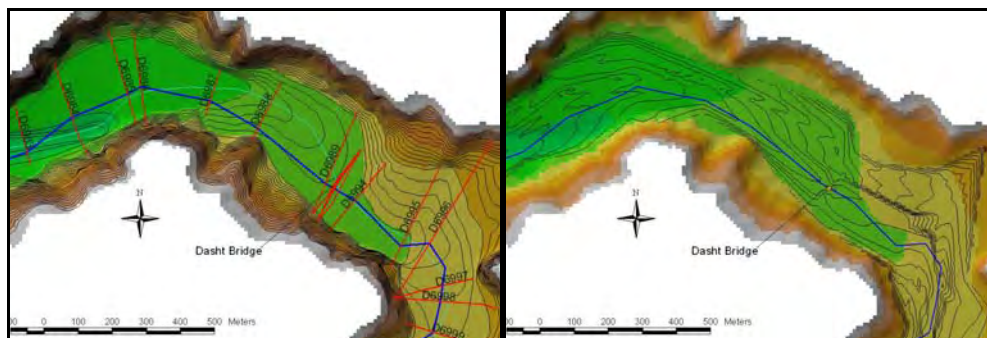


**Figure 4.12 Iran Systems DEM and contour lines. Left: Contour lines corresponding to the DEM, and Right: Contour lines generated from the MoE cross-section survey data.**

Figure 4.12 shows the DEM in the upstream end along with contour lines. To the left in Figure 4.12 the DEM is shown along with its own corresponding contour lines, while Figure 4.12 to the right shows the DEM along with contour lines generated from the MoE cross-section survey data. We make the following observations:

- The incised channel is seen to be very distinct in the survey data contour lines, which seems to be smoothed out in the DEM (along with a displacement).
- Around cross-section D6986 the DEM is completely flat, which is not reflected in the survey data.
- There is a steep ridge shown clearly along the right bank of the Madarsoo upstream of Dasht Bridge. We do not know whether this is true, but it is absent in the DEM.

#### **4.1.9 Summary**

The detailed comparison between the MoE data and the Iran Systems DEM yields many discrepancies. Here we have not even looked at elevations in detail, but merely the horizontal locations, and there are plenty of problems:

- The contours in the downstream end do not reflect the presence of an incised floodplain, which we know is there. Iran Systems have acknowledged this and promised to go out and pick up more spot elevations, with doubtful value, as their survey cannot even compete with our old 85 m grid DEM. The Iran Systems DEM should not under any circumstances be used in the downstream end.
- Further upstream the incised Madarsoo channel does not seem to be properly resolved in the DEM. Clearly the channel itself is not resolved, but this should not be a problem for low discharges where the Madarsoo has almost no size at all.
- There are plenty of discrepancies between the path of the Madarsoo according to the Iran Systems DEM and the MoE survey data. In many cases the discrepancies are huge with the river literally venturing into high ground when comparing the two data sets.

If we are to combine these two data sets, then it must be required that they correspond, which we can clearly conclude from the analysis that they do not. As was the case in earlier analyses, the discrepancies are too big for these two data sets to be used in the same model.

#### **4.2 Field trip 14 August 2005**

A field trip was conducted on 14 August 2005 with the participation of Dr. Tjerry and Mr. Momeni (interpreter, photographs and video).

The objectives of the field trip were:

- ❑ Check whether there is a bridge between 14 Metry and Kalaleh Bridges. According to Momenei there should be a bridge “Ajen Ghare Khajeh” around (370,600 m; 4,135,200 m); there were pictures taken of this bridge, but no GPS location.
- ❑ Inspect the first bridge in Golestan Forest (from Tangrah).
- ❑ Check other bridges along the way.
- ❑ Obtain the location of the Madarsoo River in the downstream end along with estimated water levels (by GPS).
- ❑ Obtain water levels as well as spillway levels in the reservoir to use for estimation of the error in the GPS elevations. This will allow a more accurate determination of the correct water levels and hence topography in the downstream end of the Madarsoo.
- ❑ We also wanted to obtain the correct location of the river in the upstream part of Golestan Forest where the DEM and the survey data are very inconsistent. However, the road through Golestan Forest had only just been reopened, and it was only a temporary road, so we opted for doing the survey another day in the near future with a 4W car and the road in perhaps better condition. It is still very important to obtain the path of the river in this area.

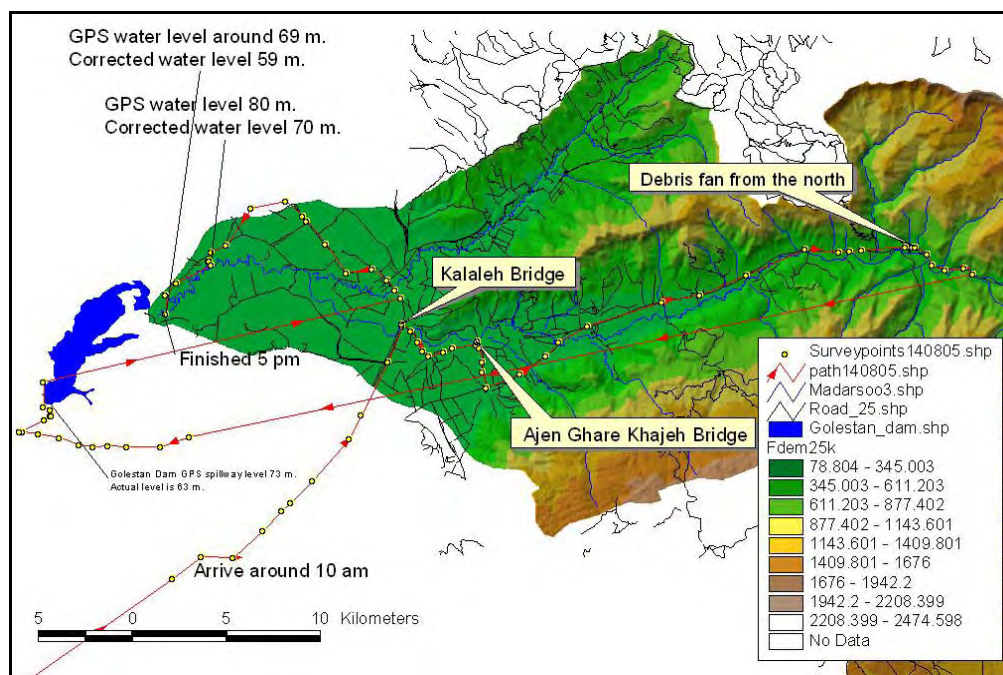


**Figure 4.13 Field trip conducted on 14 August 2005 with 82 GPS points.**

The river survey data seems to be generally accurate in the horizontal locations. However, the elevations in the downstream end cannot possibly be correct, and the explanation given by MoE in February 2005 (that the surveyed part of the river was part of the reservoir) was clearly not true. In fact, it seems in general that elevations in the downstream end go up and down almost randomly in the different data sources. This is clearly an area where we cannot trust any of the data sources. It is not known why it is so chronically difficult to measure elevations in the downstream end of Madarsoo.

#### 4.2.1 Kalaleh Road

The road from Tangrah Road up to Kalaleh Bridge was mapped with GPS on the way. The GPS mapping shows consistency between the road in shape format and the road as measured. The roads in general seem to be accurately mapped.

#### **4.2.2 Kalaleh Bridge**

We arrived at Kalaleh Bridge and took GPS points at each end. These GPS points have been taken before, but just for the fun of it. Kalaleh Bridge withstood the onslaught from the 10 August 2005 flood, and we took three photos from the bridge.

#### **4.2.3 Road from Kalaleh Bridge to Ajen Ghare Khajeh Bridge**

From Kalaleh to Ajen Ghare Khajeh Bridge was a gravel road running fairly close to and parallel to Madarsoo River. Shape files are available with this road, and we confirm the accuracy of the road path in digital form.

#### **4.2.4 Ajen Ghare Khajeh Bridge**

This bridge was not mapped in the field survey conducted 11 February 2005; it was assumed that there were no bridges between 14 Metry and Kalaleh. The existence of this bridge was confirmed, and we took the GPS point for the southern end (left bank of Madarsoo) and the middle of the bridge. The northern end of the bridge was destroyed during the flood, and a temporary road was under construction when we visited the site.

#### **4.2.5 Gravel road down to Tangrah Road from Ajen Ghare Khajeh Bridge**

This road was mapped and the mapping was found to be consistent with the existing digital format that we have for this road.

#### **4.2.6 Tangrah Road**

GPS points were taken along Tangrah road, and again we conclude that there is consistency with the road that we already have in digital form.

#### **4.2.7 Road in Golestan Forest**

GPS points were again consistent with the road that we have in digital form. The location of a debris fan was marked for future reference (MIKE 11 modeling).

#### **4.2.8 Golestan Dam**

In an attempt to reach the downstream part of Madarsoo, we ended in the downstream part of Golestan reservoir; at Golestan Dam. This turned out to not be such a bad idea after all, as we could obtain elevations of the spillway and reservoir water level. The GPS readings were:

Reservoir water level according to GPS	67 m
Spillway level according to GPS	73 m

The GPS is not very accurate on the elevation, but the error seems to be consistent and about 10 m. The actual elevation of the spillway is 63 m, and the water level is being obtained from MoE, which had not been received yet as this report was submitted.



#### 4.2.9 Downstream end of Madarsoo

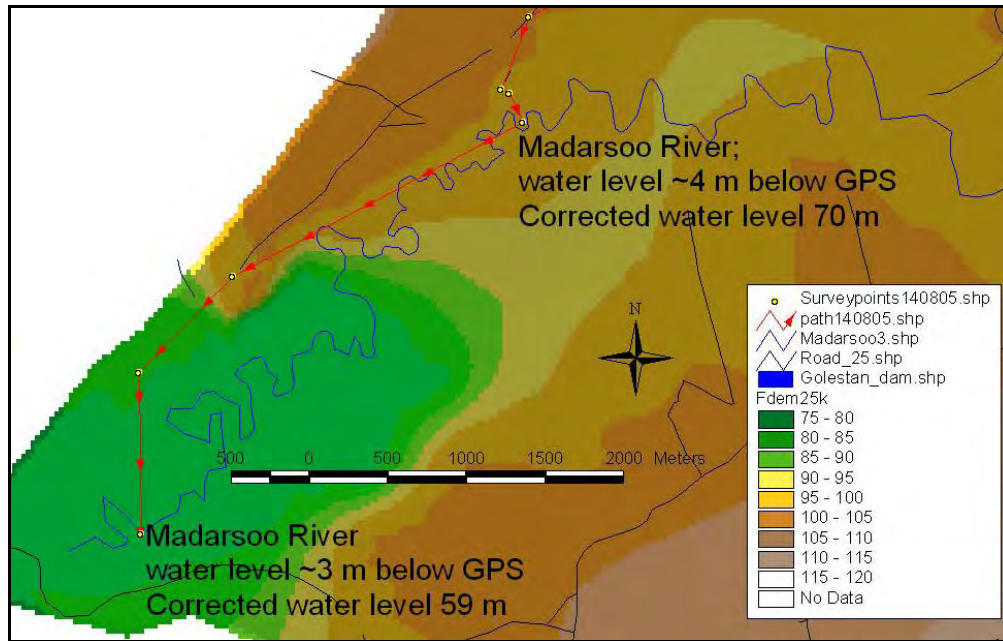


**Figure 4.14** The two elevations obtained in the downstream end of Madarsoo. The GPS locations match the surveyed river very well.

We had to turn back to Kalaleh Bridge from the Golestan Dam, cross the bridge and drive towards the downstream end of Madarsoo along the right bank of the river. The road was mapped along the way, and again we found consistency.

Two critical locations were mapped with the GPS in the downstream end, as also indicated in Figure 4.14. The water levels were estimated from the distance that the GPS was above the water surface, and corrected with the 10 m difference we found from Golestan Dam.

According to MoE (meeting 13 February 2005) both the surveyed locations are actually located in the reservoir.

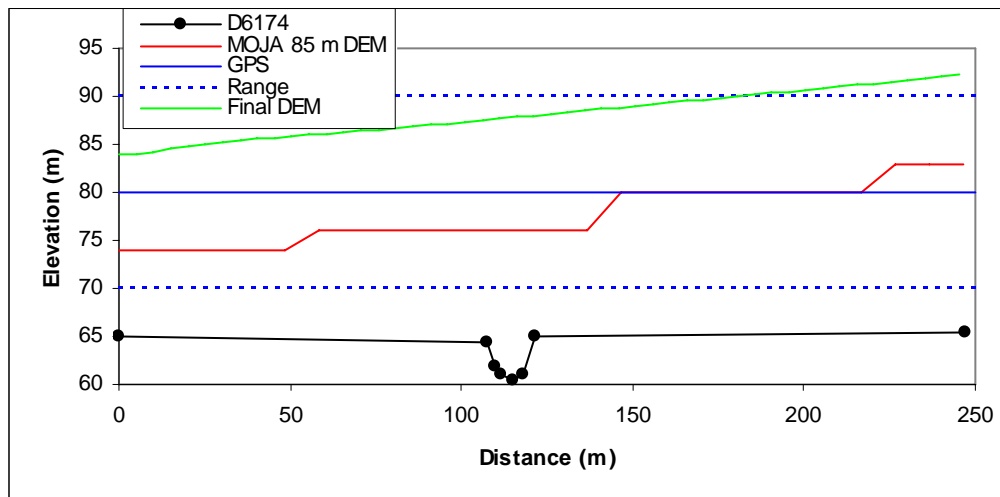


**Figure 4.15** The downstream GPS water level with +/- 10 m range, the D6174 survey cross-section at the same location, and DEM sections extracted along the survey line for the cross-section.

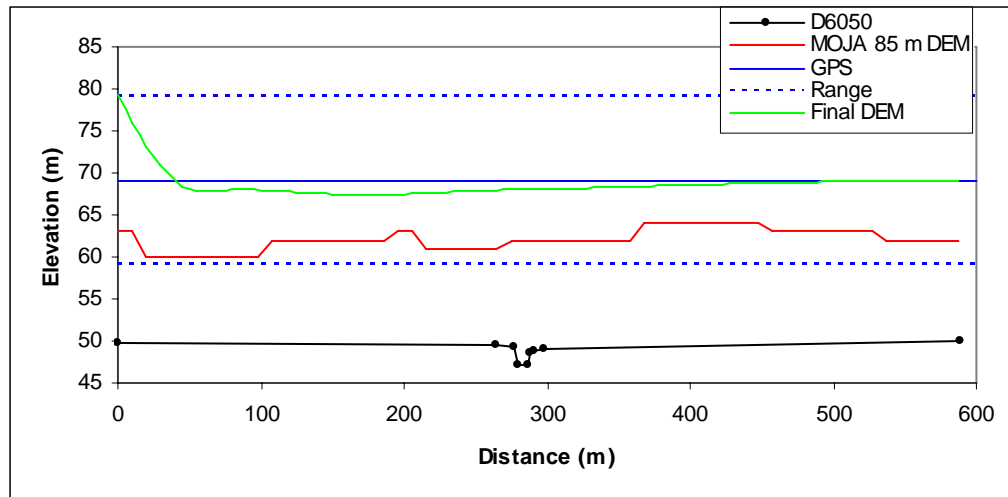


**Figure 4.16** The downstream GPS water level with  $\pm 10$  m range, the D6050 survey cross-section at the same location, and DEM sections extracted along the survey line for the cross-section.

To make things clear, we took the GPS elevations and assumed an error of  $\pm 10$  m and plotted the elevations versus cross-sections at the locations of the two survey points. The survey cross-sections D6050 and D6174 are at the locations. The following comes out clearly when investigating this.

The downstream survey section (D6050) requires that the GPS measured the water level 20 m too high in order to be correct. We were standing right next to the bank and measured the GPS elevation.

The Golestan Dam water level from 14 August will hopefully make it clear that this survey cross-section is simply wrong. In order for survey cross-section D6050 to have correct elevations, the water level in the reservoir needs to have been less than 50 m on 14 August 2005. The water level at this location may be slightly higher than the reservoir level, but there is no way it can be lower.

According to MoE this survey cross-section is in the reservoir, which makes us wonder how the channel was identified, as every single point in the cross-section would have been under water.

The most reasonable correct elevation is the GPS elevation minus 10 m, which matches up with the old DEM fairly well at both locations,

At the upstream location (D6174) the new DEM is 10 m above the upper elevation that we can reasonably assume from the GPS, and 30 m above the most likely water level. At the downstream location the new DEM can barely get into the reasonable range of the GPS and it is in the high elevation range, which is less likely than the low according to GPS measurements of Golestan Dam.

Unfortunately it has not been possible to obtain the Golestan Dam water level from 14 August, but the evidence is clear enough to conclude that the MoE cross-section survey data is erroneous.

### 4.3 Satellite imagery

Two sets of satellite imagery are available, namely a set henceforth called “742” with pixel size 28.5 m and a new Quick Bird satellite image with pixel size 60 cm. The images are shown in Figures 4.17-18.

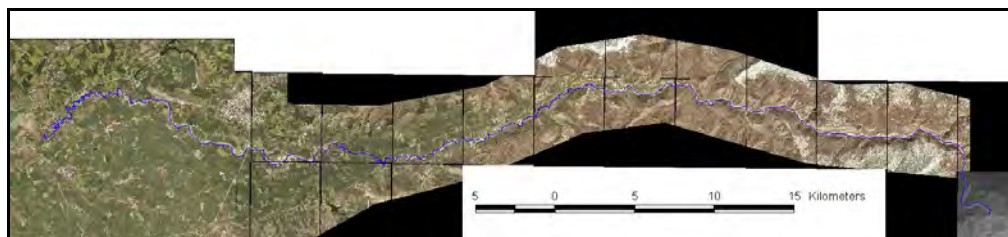


Figure 4.17 Quick Bird satellite image (pixel size 60 cm).



Figure 4.18 742 satellite image (pixel size 28.5 m)

#### 4.4 Mosaic DEM created from resampled 85 m DEM and Iran Systems DEM

The Iran Systems DEM cannot be used downstream of Kalaleh Bridge. If we chose to do so, we would get very wide flood maps with no indication of the known presence of an incised floodplain.

The DHI expert is not convinced that the Iran Systems DEM is any good upstream of Kalaleh Bridge, but we have no choice but to use it. The 85 m resampled DEM should not be used upstream of Kalaleh Bridge, as the coarse resolution will start hurting badly when the river becomes narrower.

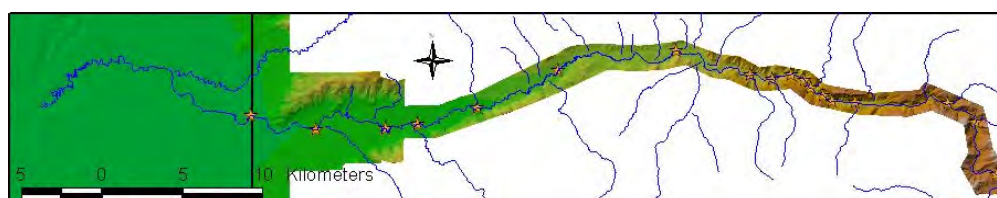


Figure 4.19 Mosaic DEM created by the resampled 85 m DEM (left of the black line) and the Iran Systems DEM (to the right of the black line).

We therefore make a mosaic DEM based on the 85 m resampled DEM and the Iran Systems DEM where the resampled DEM is used for Easting values less than 367 km (the vertical black line in the figure), as also indicated in Figure 4.19.

The DEM does not account for the Madarsoo river channel. Doing so will be very difficult with the available data, as the only source, i.e. the MoE survey data, does not match with the DEM.

It is noted that Iran Systems provided a much improved DEM in the downstream end. However, for the sake of completeness we keep this section in the report.

##### 4.4.1 Augmentation of mosaic DEM with MoE survey cross-sections

Inspection of the Iran Systems DEM shows that the DEM does not properly resolve the incised channel of the Madarsoo. In some cases it seems as if it actually does, e.g. just upstream of Kalaleh Bridge it at least looks like it, and there are other places as well. However, in general the incised channel is literally absent.

The way to go is clearly to do what has been done many times before, namely to combine the two level sources. However, this is not easy, as the two data sets match very poorly in the elevations.

The MoE cross-section data can be used for generating a surface by converting the cross-sections to xyz files, interpolate additional sections between the existing sections, create a TIN from the xyz files in ArcView and finally convert this TIN to a grid using a mask that covers the survey data.

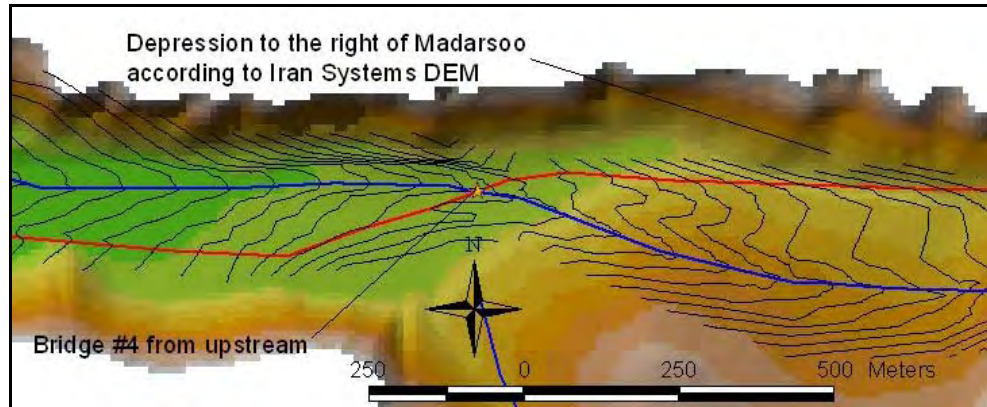


**Figure 4.20 Iran Systems DEM and contour lines created from the MoE survey cross-sections in Golestan Forest about 15 km from the upstream boundary.**

Typical variations of the MoE survey contours and the Iran Systems DEM in Golestan Forest are shown in Figure 4.20:

- The contour lines from the MoE survey data show a very well-defined Madarsoo incised channel with a width of about 100 m. The triangular shape is very clean and well-defined in most places like this, but of course the actual elevations do not match up in the two data sources; but the shape is impressively well defined in the MoE survey data.
- The incised channel is not present in the Iran Systems DEM.
- The Iran Systems DEM shows a depression to the right in the picture, which leads the Madarsoo to this location in our digitization of the river path from the Iran Systems DEM. The level in the depression is more than 20 m below the level on the hill where the Madarsoo is flowing according to the MoE data. The red line shows the road, and it is going through the depression according to the Iran Systems DEM. According to the MoE survey data, the river is going through the higher elevation area just below the depression, while the depression is actually a hill slope according to the MoE data. It is in fact possible to obtain this path of the river by lowering the topography where the MoE survey data says the river is located.

#### **4.4.2 How to “burn” the Madarsoo channel into the DEM**

Normally the procedure would be to make a grid from the survey sections, as we have already done, clip the grid to the channel (the DEM should be more reliable in the floodplain) and simply let the elevation in this grid replace the elevations in the DEM. This process is often referred to as “burning” the channel into the DEM.

“Burning” in this manner is a bad idea for the present project because the elevations in the Iran Systems DEM and the MoE survey cross-sections match up very poorly. The result would predictably be a channel that in some areas would look like a very deep canyon, and in other areas like an aqueduct.

The approach that must be followed here is to use the cross-sections to figure out how much the channel incises into the floodplain, and then subtract this from the elevation in the DEM.

Areas where the Madarsoo seems to venture into high ground will still cause problems when using this approach; we will be subtracting some meters from an already way too high elevation compared to the surroundings. Therefore it is important to ensure that the path of the river is reasonably compatible with the DEM before lowering the elevation along the path of the river.

The following need to be carried out for this task:

- ❑ Digitize the river channel and bank lines from the Quick Bird images; these images must be the most accurate source of this information. The Quick Bird images will be finalized by Mr Bai on 7 September 2005.
- ❑ Correct the path of the Madarsoo in the MoE survey data to comply with the path from the Quick Bird image. This can be done by moving each cross-section so its low point matches with the closest point in the new river path, or similarly from the bank lines.
- ❑ Ensure that the DEM complies with the path of the Madarsoo from the Quick Bird image. This is basically a test of whether there is compatibility between the DEM and the satellite images. If there is no such compatibility, it will be very difficult to carry out this task. Should this occur, we will have to move the river so the location matches with the DEM, and keep the width (important for where to burn the channel) from the Quick Bird images.
- ❑ Extracted the deepening of the Madarsoo between the two bank lines and create xyz file with this deepening. Create a TIN from the xyz file, create a grid from the TIN and clip the grid to only cover the area between the bank lines. Subtract this deepening from the DEM to represent the Madarsoo incised channel.

#### 4.5 Summary

Inconsistencies in elevation data are devastating when doing flood mapping. Indeed one can say that flood mapping based on inconsistent elevation data is a pointless exercise.

Flood mapping is a highly sophisticated technology that among other things is very unforgiving when it comes to errors in the data. Most prominent for the present situation is the reflection of the physics in the hydraulics: The water will flow in the deepest part of the valley. So when the DEM says the lowest point is somewhere else than where MoE says the river is, there will be two different river locations.

It all comes down to the statement we made in the beginning of this report: Garbage in = Garbage out. There is no hiding from reality in hydraulics; if a hydraulic model is fed garbage, it will deliver garbage.

The most important thing to get consistency between the elevation data used in the cross-sections and in the DEM. At this stage of the project this more or less means we have to use cross-sections extracted from the DEM we decide to base the flood maps on. The inconsistencies between the cross-section survey data and the DEM are simply too large. Hence we discard the cross-section survey from the project.

## CHAPTER 5 HYDROLOGY (TASK 3)

The purpose of the MIKE SHE hydrological modeling is to:

- Provide insight into the effects of vegetation on the flood hydrograph
- Provide scenario boundary conditions for the MIKE 11 HD+ST model

DHI (June 2005) analyzed and reported the effects of vegetation. Herein we describe how the results of the hydrological modeling are applied for generating boundary conditions for the MIKE 11 HD+ST model.

Boundary conditions were generated with a coupled MIKE 11/SHE model and delivered in the form of MIKE 11 result files with discharges and lateral flows.

It is not the intention to include the full network used in the MIKE 11/SHE model, just as it is not the intention to run the coupled model for anything else than the scenarios to determine boundary conditions.

In the coupled model the tributaries receive water from MIKE SHE. As we strip the MIKE SHE part from the model, we will have to replace the MIKE SHE water input by source points that are added where the tributaries join the MIKE 11 Madarsoo branch.

The following five scenarios need to be prepared for the MIKE 11 model production simulations: 2001, 2005, 25 year, 50 year and 100 year

### 5.1 Extraction of boundary conditions for the single branch MIKE 11 model

This was done by extracting discharges from the MIKE SHE result file and use them for point sources along the Madarsoo.

The MIKE 11 model starts at the Dasht village, which is handled by extracting the discharge from the first Q-point in the Madarsoo to a time-series with the inflow. This inflow is then the upstream inflow in the Madarsoo branch.

The tributaries are handled by extracting the discharge from the first Q-point upstream in the tributary and adding the lateral flow (Drain, Overland and Baseflow from MIKE SHE) into the downstream H-point in the tributary branch into a time-series file. A point source with this time-series at the junction now replaces the tributary. There are 26 such tributaries handled in this manner in the single branch MIKE 11 model.

The lateral flows from the MIKE SHE model divided into Drain, Overland and Baseflow are joining up with the Madarsoo down through the branch. These lateral flows are extracted from the result file into time-series and point sources are added to the chainage locations where these lateral flows join the Madarsoo. There are 86 of these lateral flows entering at H-points down through the Madarsoo.

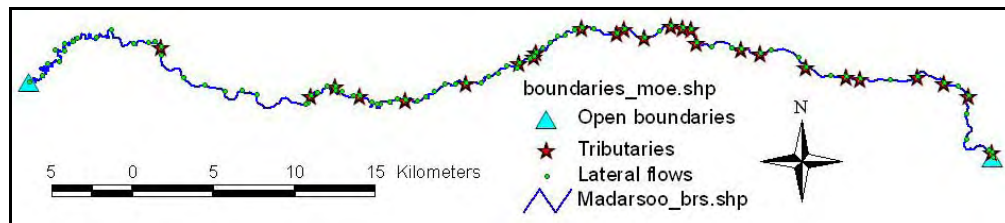


**Figure 5.1** Locations of the boundary conditions extracted from the MIKE 11/SHE model. Each boundary condition has a location and an associated discharge time-series for each of the five scenarios.

Figure 5.1 shows the locations of the boundary conditions along the MoE survey data based network.

### 5.1.1 Translation to a different network

Changes are likely to be made to the network for two reasons:

- The network obtained from the MoE data does not match with the Iran Systems DEM
- The network should reflect the path of the floodwater rather than the meandering path of the Madarsoo.

The transformation of the MIKE 11/SHE coupled model results was made so the transformation allows a different network to be specified in the output of time-series and MIKE 11 boundary (source points) specifications. The method is simply to calculate the geographical location of each source point from the branch and chainage, and then find the nearest cross-section location in the modified network.

## CHAPTER 6 DEBRIS FLOW (TASK 4)

Takahashi (1991) gives the theoretical background for debris flow, but for the practical application in this project a literature search using Google was preferred.

The objectives are to produce debris flow time-series for use in sediment point sources in the MIKE 11 ST model, while the particle size distribution was already determined from the sediment samples in Phase 1 (DHI, February 2005). To achieve the objectives the following tasks needed to be carried out:

Identify all tributaries that can produce debris flow.

For each debris flow prone tributary, determine a debris flow time-series (sediment transport,  $m^3/s$ ) using an accepted method.

Add the debris flow time-series to a point source in the MIKE 11 ST model.

Figure 6.1 shows the eleven locations where debris flow took place during the 2001 flood. These eleven tributaries were selected as debris prone, and debris flow time-series will be calculated for each tributary.

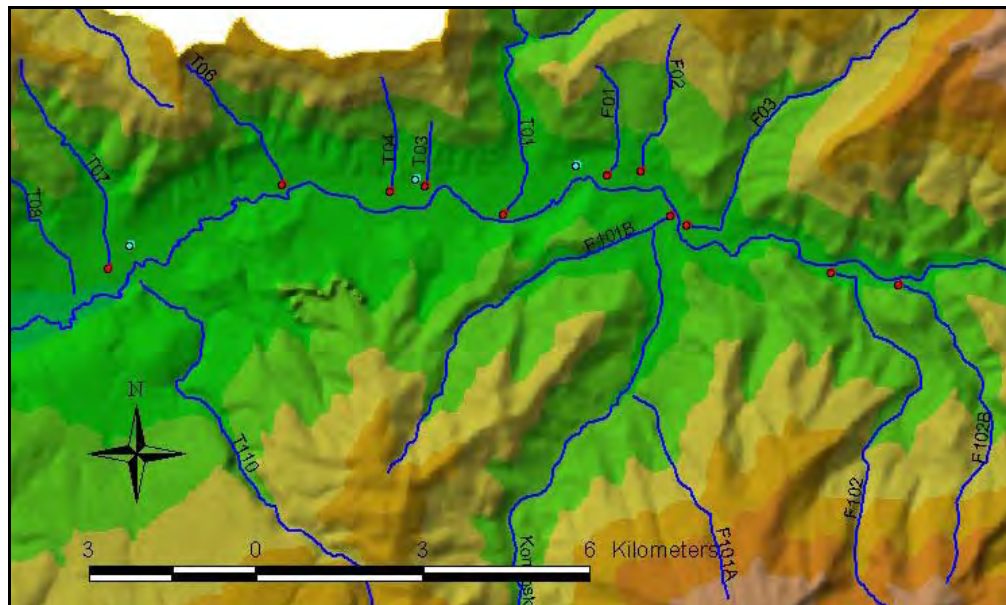


**Figure 6.1** The eleven locations with debris flow observed during the 2001 flood (red circles), and the corresponding tributaries, along the left bank F102B, F102, F101B/F101A/Kondoskooch and along the right bank F03, F02, F01, T01, T03, T04, T06 and T07.

For the debris location at the junction with Kondoskooch River we will assume that the debris flow takes place in the F101B tributary, and for T01 and T02 we will assume that the debris flow originates in T01. However, for the sake of completeness we calculate the debris flow for all relevant tributaries in the debris flow range, except for Kondoskooch River.

### 6.1 Calculation of the debris yield using the Los Angeles District Debris Method

The Los Angeles District (February 2000) debris yield formula is given for different catchment areas, but most of the debris flow prone tributaries fall within the 3-10  $mi^2$  (7.8-25.9  $km^2$ ) range where the formula is given by:



$$\log_{10} Dy = 0.85 \log_{10} Q + 0.53 \log_{10} RR + 0.04 \log_{10} A + 0.22 FF$$

Where:

- Dy Debris yield (yd<sup>3</sup>/mi<sup>2</sup>)
- Q Unit peak runoff (ft<sup>3</sup>/s/mi<sup>2</sup>)
- RR Relief ratio (ft/mi)
- A Drainage area (acres)
- FF Fire factor

The formula can be rewritten into the perhaps easier to understand expression:

$$Dy = 1.66^{FF} Q^{0.85} RR^{0.53} A^{0.04}$$

The expression does not imply a highly non-linear phenomenon; the debris flow is close to (not even) proportional to the discharge, which is the only parameter that will vary between different scenarios (same slope, drainage and fire factor). The US Army Corps points out that the formula is only fully valid for California. However, we will assume that the order of magnitude is accurate enough for Madarsoo river basin.

The formula is only valid for drainage areas 3-10 mi<sup>2</sup>. A separate formula is given for watersheds smaller than 3 mi<sup>2</sup>, but it is based on the maximum 1-hour precipitation rather than the unit discharge, and we know almost nothing about the maximum 1-hour precipitation. Therefore we will allow the 3-10 mi<sup>2</sup> formula to be applied for all watersheds in the catchment.

The Fire Factor is very important for debris flow in California. We will assume that fire has no impact on the debris flow in the Madarsoo river basin, which is reasonable, and use a fire factor of 3 everywhere (3 seems to be the lowest value). The Fire Factor can vary from 3-6, and the equation shows that a Fire Factor of 4 yields 1.66 (10<sup>0.22</sup>) times more debris flow than a Fire Factor of 3.

As is also evident from the Los Angeles Debris Method the primary factors in the debris yield are the peak discharge and slope. Translating this to the Madarsoo River we find that the debris prone tributaries are concentrated in the area with intense rainfall and high slope.

**Table 6.1 Calculated debris yields (2001 flood) for the selected debris flow prone tributaries.**

Drainage	2001 peak (m <sup>3</sup> /s)	Area (km <sup>2</sup> )	Max elev. (m)	Min elev. (m)	Length (m)	Yield (m <sup>3</sup> )
F102B	25	13.7	1,680	578	6,876	70,557
F102	31	12.7	1,943	546	8,717	83,524
F03	31	16.1	1,870	498	8,390	88,306
F02	8	4.9	1,092	500	3,119	24,099
F01	6	2.9	913	487	2,311	16,838
T03	2	0.5	714	432	1,242	5,287
T04	4	2.1	1,078	423	2,401	13,807
T06	7	3.6	1,150	389	3,301	22,501
T07	9	8.1	1,080	369	4,671	26,079
T02	34	23.9	1,448	600	8,737	78,098
T01	32	28.5	1,447	440	12,835	68,507
F101B	26	10.0	1,270	488	7,807	53,596
F101A	15	6.6	1,806	620	4,698	50,641

The formula was applied for the 2001 flood in which we extracted the peak flow from the MIKE 11 hydraulic results, estimated the catchment area in ArcView, and found the elevations and length in the MIKE 11 network. The data was inserted into a spreadsheet, and the debris yield was calculated for each of the tributaries.

**Table 6.2** Calculated debris yield for each of the selected debris prone tributaries for the five different events (2001, 2005, 25, 50, 100 year).

Drainage	25 year (m <sup>3</sup> )	50 year (m <sup>3</sup> )	100 year (m <sup>3</sup> )	2001 (m <sup>3</sup> )	2005 (m <sup>3</sup> )
F102B	55,877	67,426	82,385	70,557	50,836
F102	64,807	80,537	98,861	83,524	60,712
F03	68,517	84,660	102,637	88,306	63,675
F02	18,871	24,610	30,366	24,099	18,871
F01	14,421	18,023	21,731	16,838	13,434
T03	4,140	5,197	6,391	5,287	3,904
T04	10,812	14,392	17,819	13,807	11,117
T06	18,330	23,318	29,430	22,501	17,762
T07	20,550	25,338	31,645	26,079	19,777
T02	61,156	75,356	92,138	78,098	56,848
T01	53,646	66,682	81,757	68,507	50,398
F101B	42,883	52,543	64,620	53,596	40,317
F101A	41,892	51,501	62,741	50,641	38,605

The resulting debris yields for the 2001 flood are shown in Table 6.1. The debris yield ranges from 5-88 thousand m<sup>3</sup>, where the upper values of the yield correspond to what we have calculated that the debris yield should be to have a significant impact on the Madarsoo flood maps.

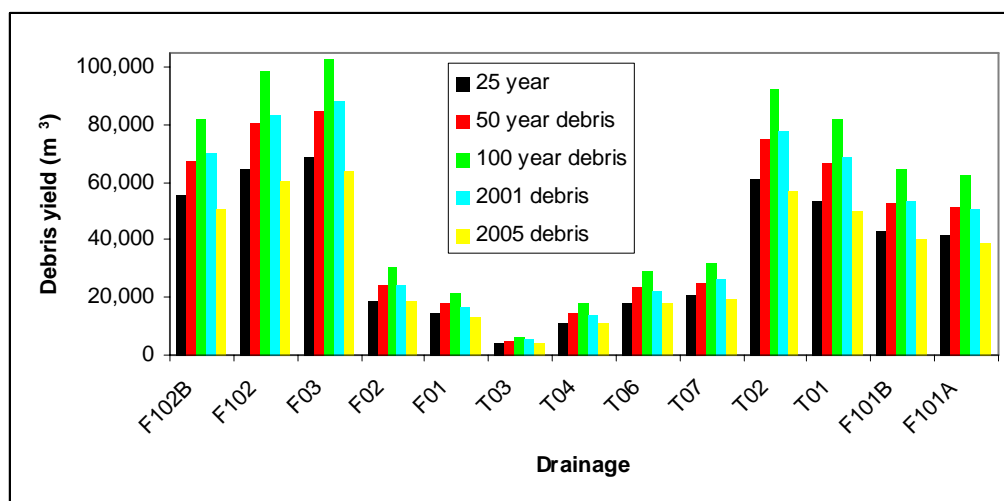


**Figure 6.2** Debris yield for each drainage for the five scenarios (2001, 2005, 25, 50, 100 year).

Table 6.2 shows the tabulated debris yields for each tributary and each scenario, while the same is shown in a bar graph in Figure 6.2.

## 6.2 Distribution in time of the debris flow

The distribution in time can be modeled in two ways:

- By assuming a relation to the tributary discharge, i.e.  $Q_{\text{debris}} = f(Q_{\text{water}})$
- By using a model function, e.g. debris flow takes place with constant rate over one hour.

We have not yet decided how to do this. The distribution in time has some influence on how much the debris flow will impact flooding; clearly a debris flow very concentrated in time will result in more flooding, but it should also be realistic.

For the present preliminary model we have used a simple scaling method in which the debris flow rate is assumed to be a function of the hydrograph in the following manner:

$$Q_s(t) \approx \max(0, \frac{Q(t) - aQ_{\max}}{(1 - a)Q_{\max}})$$

Where  $Q_{\max}$  is the peak discharge and  $Q(t)$  the hydrograph. This is simply a scaling where we assume that the debris flow is proportional to the discharge minus “a” times the peak discharge; it concentrates the debris flow in the time period where the discharge is above “a” times the peak flow. The maximum of the given function is unity (when  $Q(t)=Q_{\max}$ ), and the debris flow rate is scaled to match the debris yield.

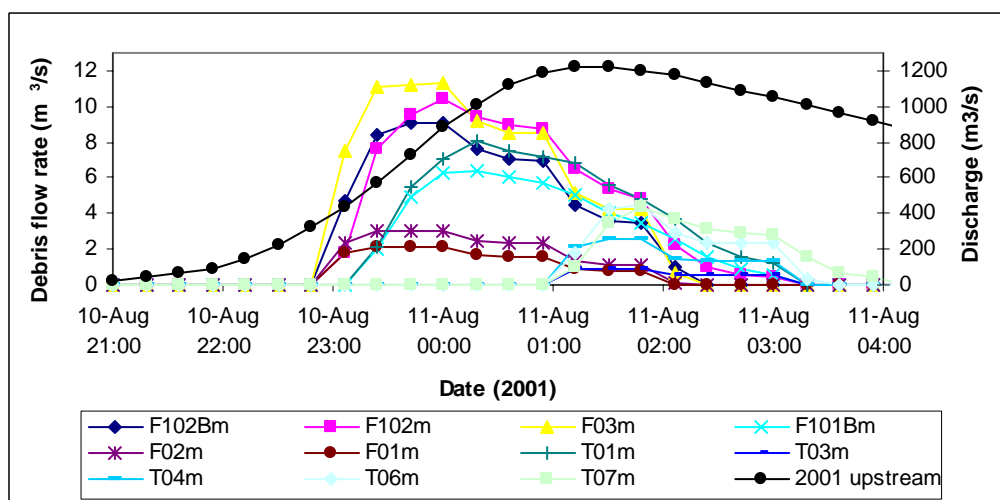


**Figure 6.3 Debris flow rates calculated with a=0.8 for the 2001 flood.**

The debris flow time-series calculated with the method are shown for the 2001 flood in Figure 6.3. It is seen that the debris flow rate goes up to about 11 m<sup>3</sup>/s, which is of course for the F03 tributary.

The inflow at the upper boundary (Dasht) is also shown for reference. The timing is seen to be difference, which has important implications for how to model the debris deposits, which is explained in a later section.

### 6.3 Particle size distribution of the debris flow

We will assume that the debris flow has the average particle size distribution that we found from the analysis of the sediment data (JWRC, 2004), which resulted in:

- 58% sand 0.17 mm
- 42% gravel 54 mm

These were also reported by DHI (February 2005).

For the present application the debris is assumed to be only the coarse sediment, while the fine fraction is available in the river channel.

### 6.4 Timing of the debris flow and the Madarsoo hydrograph

During this second phase of the study it has become clear that the debris flow prone tributaries in the Tangrah area have their peak about 2 hours before the Madarsoo, see Figure 6.3. This has major implications for how to model the debris flow.

The first point we need to make clear is that the debris flow will surely be timed with the flow in the tributary in which it originates. Therefore the debris flow will take place before the Madarsoo discharge peaks, and hence there will be a deposit of rocks and boulders created in the river valley before the Madarsoo hydrograph arrives.

As described by DHI (February 2005) the grid spacing is not important, as long as the grid is fine enough, when the debris deposit is eroded right when it enters the Madarsoo. The reason is that the local sediment transport will instantly adjust to be able to transport the debris flow due to the lower water depth (that will keep decreasing until the transport capacity is up to the debris inflow).

However, the situation is different than anticipated. The debris deposit is not eroded immediately because the Madarsoo discharge is still fairly low when the debris flow arrives. The debris deposit is therefore not likely to be eroded much initially, and therefore the grid spacing will have a decisive impact on the height of the debris deposit.

What is missing here is the initial longitudinal shaping of the deposit. Clearly the debris will not form a tower with the width (W) of the river, a longitudinal extend equal to the grid spacing ( $\Delta x$ ), and a height of  $H = \text{Volume} / (W \cdot \Delta x)$ , as will be the case when the debris deposit is added as a point source. For a grid spacing of 10 m and a width of 200 m, a debris deposit of 100,000 m<sup>3</sup> would be 50 m tall. Again, this would not be an issue if the debris flow was timed with the Madarsoo hydrograph, as we demonstrated earlier.

There is also a numerical perspective involved here. The simulations with all debris flow added to one single point show the debris input literally acts as a shock in the numerical solution, and it was very difficult to avoid this behavior. The tendency was that the debris would form a plug that the river could not follow and the result would be no sediment transport locally at the debris deposit and hence the deposit would grow and grow. This is a numerical problem, but it is nonetheless very relevant in the model application.

Physically it is not reasonable to have a deposit that is only ( $\Delta x =$ ) 10 m wide, as the width of the tributary itself will distribute the sediment longitudinally in Madarsoo along with sliding of the sediment.

#### 6.4.1 Longitudinal distribution of the debris

A reasonable shape of the debris deposit is a triangular shape in the longitudinal direction with height H, width W and length L. The volume of the debris deposit hence becomes:

$$Vol = \frac{1}{2}HWL$$

The Length/Height ratio is now called  $\alpha$ , and we rewrite the equation into:

$$H = \sqrt{\frac{2Vol}{\alpha W}}$$

It is the Length/Height ratio that becomes unrealistic when adding all the sediment to a single point when the grid spacing is low (which it needs to be). Therefore we now instead take direct control of the Length/Height ratio.

In the following the formula is applied for all the debris tributaries in an iterative calculation.

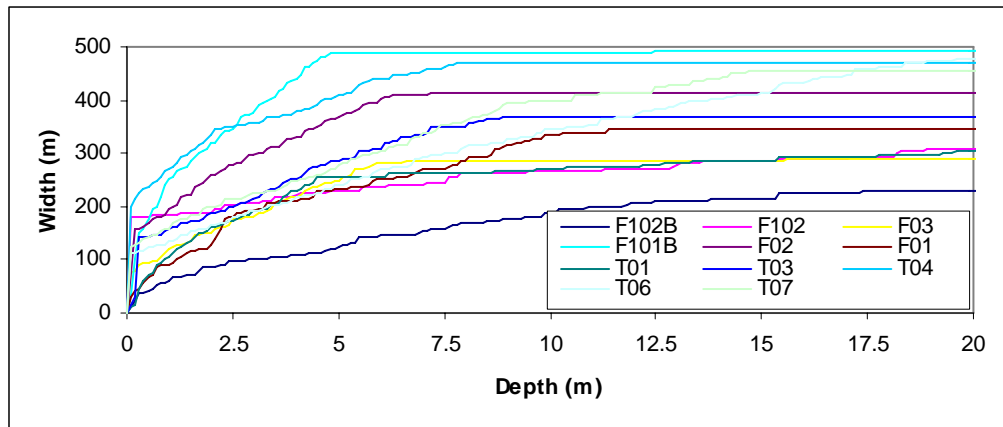


**Figure 6.4** Depth-Width curves for the cross-sections that the debris prone tributaries enter in the Madarsoo network (Iran Systems version).

The width is determined from the cross-sections located at the connections to the Madarsoo. Figure 6.4 shows the depth-width curves for all these sections. The width is calculated as function of the height (=depth) of the debris deposit, which requires iteration:

$$H = \sqrt{\frac{2Vol}{\alpha W(H)}}$$

It is not fully correct to assume that the maximum depth is equal to the height of the debris deposit (only true for a rectangular cross-section shape). The purpose here is, however, to distribute the debris volume over a distance, while the actual height is of less importance (it will come out from the model).

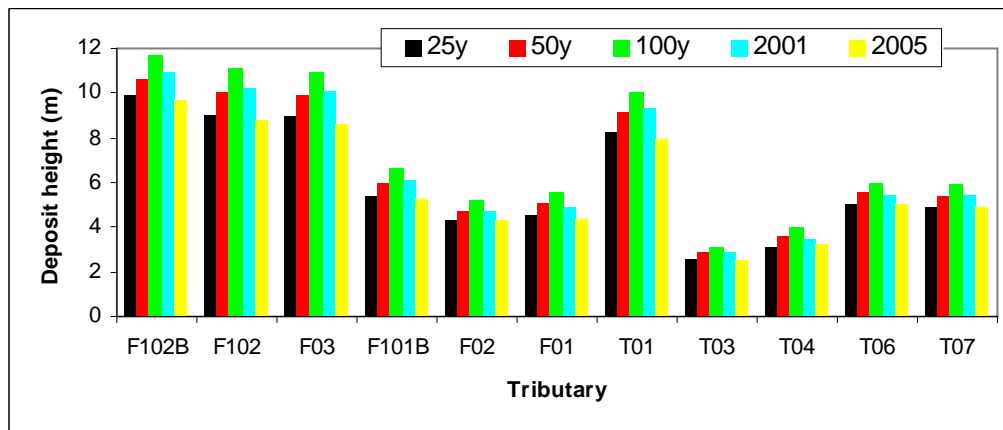


**Figure 6.5** Calculated height of the debris deposit for each tributary for all five scenarios by assuming a triangular shape ( $\alpha = 6$ ).

Figure 6.5 shows the calculated heights of the debris deposits with a triangular shape (all tributaries and all five scenarios). It is again noted that this is not the height that the debris deposit will reach; it will be used for calculating a distribution function.

The length of the debris deposit is given by  $L = H$ , which shows that the length will vary from about 20-70 m for the triangular shaped deposits, which also seems like a very reasonable range considering the width of the tributaries. With a grid spacing of 10 m it means the debris should be distributed over 2-7 grid points, i.e. 2-7 point sources. In order to achieve some uniformity in handling this many point sources, each debris inflow is distributed over 5 grid points with a distribution key explained in the following.

In the central source point the debris inflow is simply:

$$V_0 = \max(Vol, H\Delta x W)$$

In other words the volume that matches the height of the triangle over the length  $x$ , not to exceed the total volume. This is then subtracted from the total volume, and the remaining volume is distributed among the five remaining grid points with  $1/3$  in each of the two grid points adjacent to the central point and  $1/6$  in each of the two outer grid points ( $1/3+1/3+1/6+1/6=1$ ). The actual distribution key is not as important as the fact that we have now distributed the debris inflow over some distance.